Second Simulation of the Satellite Signal in the Solar Spectrum (6S)

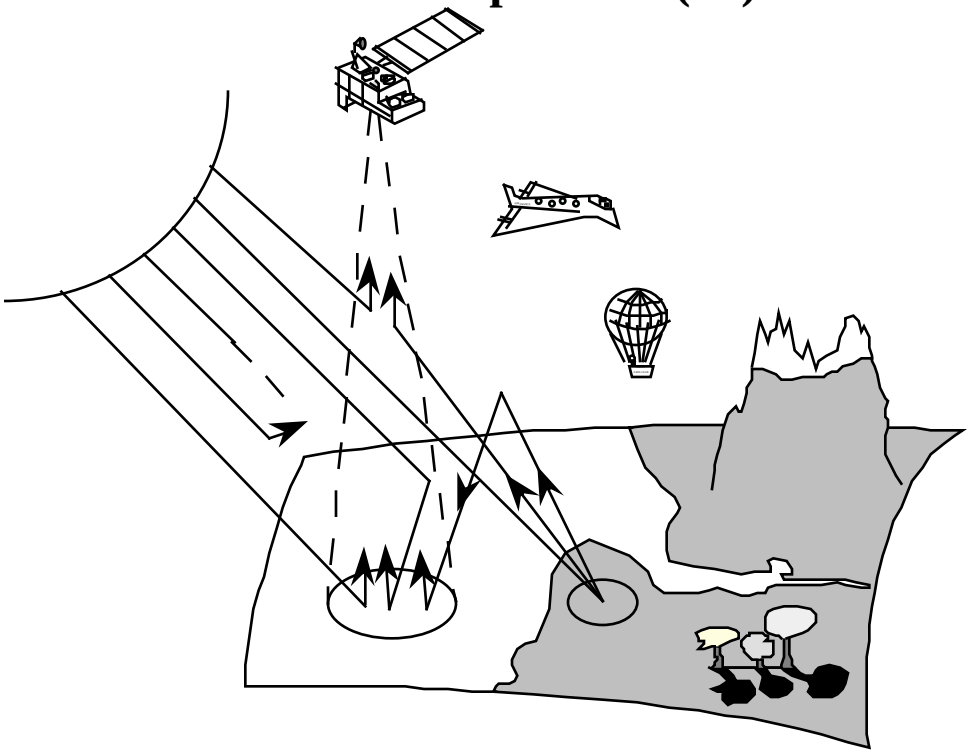

Vermote E.[1,*], Tanré D.[2], Deuzé J. L.[2],
Herman M.[2], and Morcrette J. J.[3]

(1) *Department of Geography, University of Maryland*
address for correspondence:
NASA-Goddard Space Flight Center-Code 923
Greenbelt, MD 20771, USA

(2) *Laboratoire d'Optique Atmosphérique, URA CNRS 713*
Université des Sciences et Technologies de Lille
59655 Villeneuve d'Ascq Cédex, France

(3) *European Centre for Medium Range Weather Forecast*
Shinfield Park, Reading
Berkshire RG2 9AX, United Kingdom

[*] *Formerly affiliated to Laboratoire d'Optique Atmosphérique*

Contents

ABSTRACT

The remote sensing from satellite or airborne platform of land or sea surface in the visible and near infrared is strongly affected by the presence of the atmosphere on the Sun-target-Sensor path. The following manual presents 6S (Second Simulation of the Satellite Signal in the Solar Spectrum), a code enabling simulations of the above problem. The 6S code is the improved version of 5S developed by the Laboratoire d'Optique Atmospherique, 10 years ago. It enables to simulate plane observations, to account for elevated targets, to take into account non lambertian surface boundary conditions, and new gases (CH_4,N_2O,CO) have been integrated in the computation of the gaseous transmission. The computation accuracy regarding Rayleigh and aerosol scattering effects has been improved by the use of state of the art approximation and use of the successive orders of scattering method. The step used for spectral integration has been improved to 2.5 nanometers. Finally, all community approved results (e.g.: computation of Rayleigh optical depth) have been integrated in the code.

INTRODUCTION

In the solar spectrum, sensors on meteorological or Earth remote sensing satellites measure the radiance reflected by the atmosphere-Earth surface system illuminated by the sun. This signal depends on the surface reflectance, but it is also perturbed by two atmospheric processes, the gaseous absorption and the scattering by molecules and aerosols.

In the ideal case (without interfering atmosphere), the solar radiation illuminates the surface. A fraction of the incoming photons is absorbed by the surface, whereas the remaining photons are reflected back to space. Therefore, the measured radiance directly depends on the surface properties: this radiance is the useful signal as much as it characterizes the actual surface reflectance.

In the actual case, the signal is perturbed by the atmosphere. Only a fraction of the photons coming from the target reaches the satellite sensor, typically 80% at 0.85μm and 50% at 0.45μm, so that the target seems less reflecting. The missing photons have been lost through two processes: absorption and scattering.

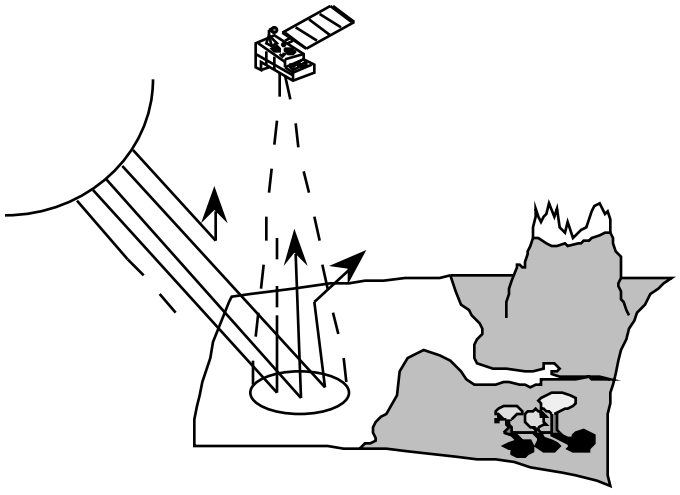

Some photons have been absorbed by aerosols or atmospheric gases (principally O_3, H_2O, O_2, CO_2, CH_4 and N_2O). Generally, absorption by aerosols is small, and satellite sensor channels avoid the molecular absorption bands. Thus, in this study, the absorption effect is a correction factor. Nevertheless, we have corrected for the absorption as accurately as possible which allows

this code to be used to help to define new satellite sensor spectral channel. The absorption is computed using statistical band models with a $10cm^{-1}$ resolution.

While some photons are absorbed others are scattered. The interaction with molecules or non-absorbing aerosols is elastic, and the photons are immediately re-emitted in a direction other than the incident one. After one or several such scattering processes, these photons leave the atmosphere and must be counted in the budget of photons reaching the satellite sensor. However, their paths are more complex than the previous direct paths as explained hereafter.

Firstly, let us consider the photons coming from the sun and scattered by the atmosphere on the Sun-surface path :
– Some of them do not reach the surface and are backscattered toward the space. They take part in our radiative balance. This signal is an interference term; it does not carry any information about the target.

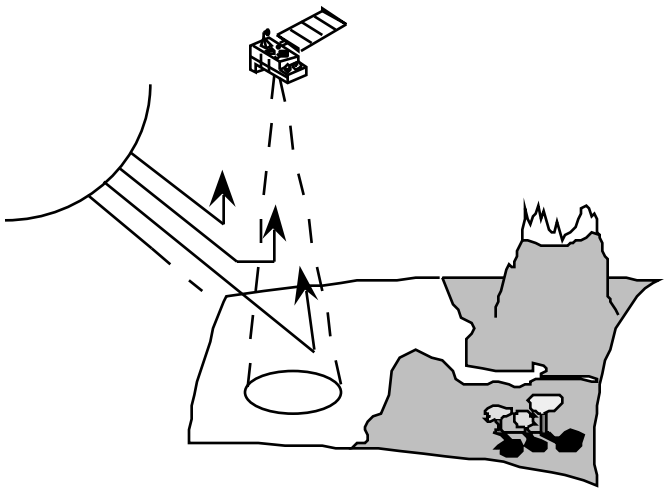

– The remaining photons contribute to the illumination of the ground by the way of scattered paths and compensate the attenuation of the direct solar paths. This diffuse component has therefore to be considered in the useful signal.

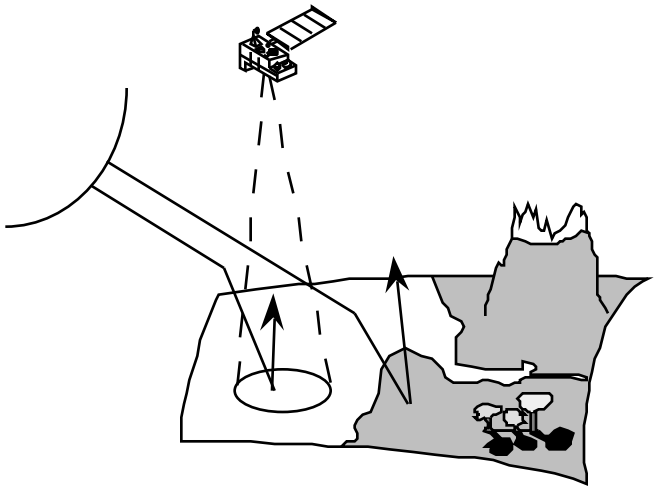

In a second step, let us consider the photons reflected by the surface and scattered by the atmosphere on the surface-satellite path. By the same way, a fraction will be scattered toward the sensor. This component has to be carefully considered. If the surface is uniform, it is an useful component but if the surface has a patchy structure, this term will introduce environment effects that will be a perturbation.

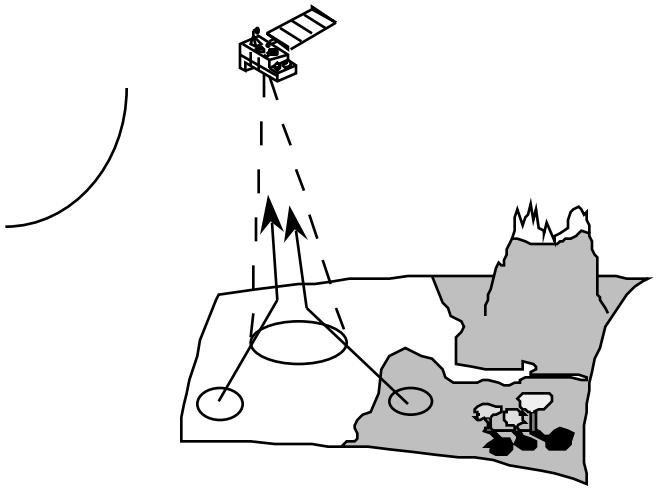

Finally, a fraction of the photons reflected by the surface will be backscattered by the atmosphere to the surface and will create a third component of its illumination ; it is the trapping effect, the photons successively interact with the surface and the atmosphere but, generally, the convergence is fast and after one or two interactions, the phenomenon can be neglected.

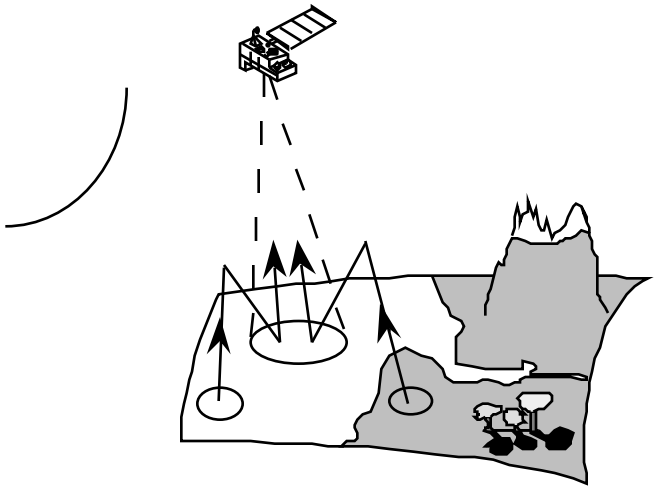

From this qualitative description, we can then infer a modeling of the atmospheric effects based upon:

- an accurate approach of the absorption by atmospheric gases
- a complete treatment of the scattering processes
- and an approximation for the interaction between the two processes.

DESCRIPTION OF THE ATMOSPHERIC EFFECTS IN SATELLITE OBSERVATIONS

1 *Absorbing effects*

In the solar spectrum the atmospheric gaseous absorption is principally due to:

- oxygen (O_2);
- ozone (O_3);
- water vapor (H_2O);
- carbon dioxide (CO_2);
- methane (CH_4);
- nitrous oxide (N_2O).

O2, CO2, CH4, and N2O are assumed constant and uniformly mixed in the atmosphere, H2O and O3 concentrations depend on the time and the location. The latter two are the most important gases in our study.

Gases absorb the radiation by changes of rotational, vibrational or electronic states. The variations of rotational energy are weak and correspond to the emission or to the absorption of photons of weak frequency, which are then located in microwave or far-infrared range. The vibrational transitions correspond to greater energy which open to absorption spectrum in the near infrared. They can also take place with rotational transitions and then give rise to vibrational-rotational bands. Lastly, electronic transitions correspond to more important energy and give rise to absorption or emission bands in the visible and the ultra-violet range. Since these transitions occur at discrete values, the absorption coefficients vary very quickly with the frequency and present a very complex structure.

Once the position, intensity and shape of each line in an absorption band is known, the absorption can be then exactly computed using line-by-line integrations. Such a model requires a very large computational time which makes it necessary to use an equivalent band model. We have divided the solar spectrum into spectral intervals of $10 cm^{-1}$ width using HITRAN database. This width allows a good description of the spectral variations of the transmission and of the overlapping between absorption bands of different gases. Moreover, this allows enough absorption lines to be contained in order that the transmission models remain well adapted to the problem.

We chose two random exponential band models, Goody (1964) for H_2O and Malkmus (1967) for the other gases. When several gases present absorption bands, we put the total transmission as the product of each gas transmission.

A complete description of the statistical models is given in Appendix III (subroutine ABSTRA), Here we present the results for each gas between 0.25μm and 4μm for a standard atmosphere model corresponding to the US-1962 standard atmosphere and a sun at the nadir (air mass is 1.0). These resuts are depicted in Figures I-1 to I-6.

The H_2O contribution (Fig. I-1) affects mainly wavelengths greater than 0.7μm. On the other hand, O_3 presents a significant absorption between 0.55 and 0.65μm and limits the earth observations at wavelengths less than 0.35μm (Fig. I-2). The CO_2 contribution occurs beyond 1μm, but more weakly than H_2O and only perturbing the water vapor windows (Fig. I-3). The O_2 influence is limited to a very strong band about 0.7μm (Fig. I-4). The CH_4 presents two absorption bands at 2.3 and 3.35μm (Fig. I-6). Finally, the N_2O contribution appears in two bands at 2.9 and 3.9μm (Fig. I-5).

In summary, we have, in the Solar Spectrum, good atmospheric windows for terrestrial observations by satellites :

- in the visible: between 0.40 and 0.75μm
- in the near and middle infrared: at about 0.85, 1.06, 1.22, 1.60, 2.20μm.

Fig. I-7 to I-14 display these windows.

2 ***Scattering effects***

2.1 Case of a Lambertian uniform target

In a first step, assuming that the surface is of uniform Lambertian reflectance and the atmosphere horizontally uniform and various, the measured quantities will be expressed in terms of equivalent reflectance, ρ^* defined as:

$$\rho^* = \frac{\Pi\, L}{\mu_s\, E_s} \qquad (1)$$

with L the measured radiance, E_S the solar flux at the top of the atmosphere and $\mu_S = cos(\theta_S)$ where θ_S is the sun zenith angle.

The optical thickness of the atmosphere will be noted τ, the viewing direction will be referenced by the zenith angle θ_V and the azimuth angle ϕ_V, and the sun angles by θ_S and ϕ_S. ρ_t will be the reflectance of the target. Absorption problems will not be considered in this part.

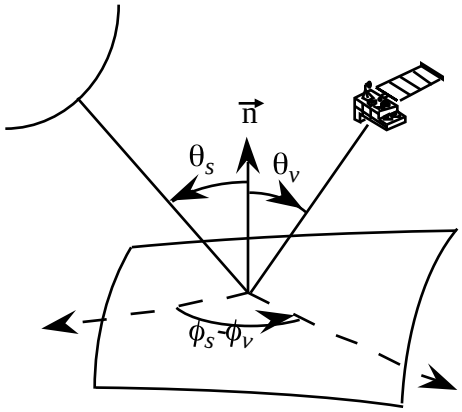

It is convenient to express the signal received by the satellite as a function of successive orders of radiation interactions in the coupled surface-atmosphere system.

For the surface illumination, we have by decreasing magnitudes :

• the downward direct solar flux attenuated by the atmosphere E_{sol}^{dir}

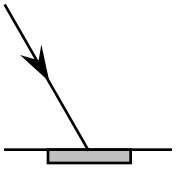

$$E_{sol}^{dir} = \mu_s E_s e^{-\tau/\mu_s}$$

• the downward diffuse solar irradiance E_{sol}^{diff} ; it is independent from surface properties and will be noted by a diffuse transmittance factor $t_d(\theta_S)$ defined as

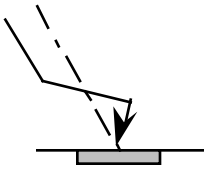

$$t_d(\theta_s) = \frac{E_{sol}^{diff}(\theta_s)}{\mu_s E_s}$$

• a second scattered flux due to the trapping mechanism; it is depending on the environment of the target and corresponds to the successive reflections and scattering between the surface and the atmosphere. If the spherical albedo of the atmosphere is noted *S*, we can write this terms as :

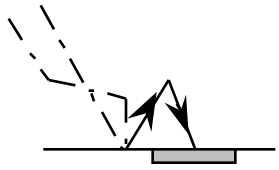

$$\left[e^{-\tau/\mu_s} + t_d(\theta_s) \right] \left[\rho_t S + \rho_t^2 S^2 + ... \right]$$

The total normalized illumination at the surface level is then written :

$$T(\theta_s)/[1 - \rho_t S] \qquad (2)$$

where $T(\theta_S)$ is the total transmittance :

$$T(\theta_s) = e^{-\tau/\mu_s} + t_d(\theta_s) \qquad (3)$$

At the satellite level, the radiance results from :

• the contribution of the total (direct plus diffuse) solar radiation reflected by the surface and directly transmitted from the surface to the sensor expressed by $e^{-\tau/\mu_v}$ with $\mu_v = cos(\theta_v)$

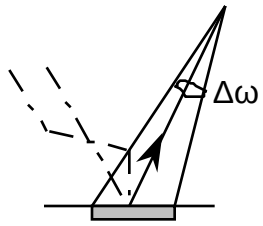

• the intrinsic atmospheric radiance expressed in terms of reflectances by function $\rho_a(\theta_s,\theta_v,\phi_S-\phi_V)$

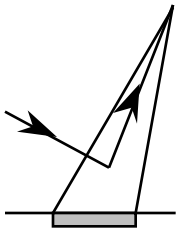

• the contribution of the environment which reflects the total (direct + diffuse) downward flux, the photons reaching the sensor by scattering ; we note this new atmospheric diffuse transmittance $t_d'(\theta_v)$

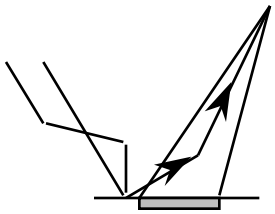

So, the apparent reflectance ρ* at the satellite level can be expressed as

$$\rho^*(\theta_s,\theta_v,\phi_s-\phi_v) = \rho_a(\theta_s,\theta_v,\phi_s-\phi_v) + \frac{T(\theta_s)}{1-\rho_t S}(\rho_t e^{-\tau/\mu_v} + \rho_t t_d'(\theta_v)) \quad (4)$$

In actual fact, the functions $t_d(\theta_s)$ and $t'_d(\theta_v)$ are identical in accordance with the reciprocity principle and ρ* can be rewritten

$$\rho^*(\theta_s,\theta_v,\phi_s-\phi_v) = \rho_a(\theta_s,\theta_v,\phi_s-\phi_v) + \frac{\rho_t}{1-\rho_t S}T(\theta_s)T(\theta_v) \quad (5)$$

with

$$T(\theta_v) = e^{-\tau/\mu_v} + t_d(\theta_v) \quad (6)$$

2.2 Environment function

Let us assume that the surface reflectance is now not uniform. In a first approach, we shall consider a small target *M* of reflectance $\rho_c(M)$ with an uniform environment of reflectance $\rho_e(M)$. In this case, Eq.(4) remains interesting by its formalism, it gives the weight of each reflectance and ρ^* can be now written as

$$\rho^*(\theta_s,\theta_v,\phi_s-\phi_v) = \rho_a(\theta_s,\theta_v,\phi_s-\phi_v) + \frac{T(\theta_s)}{1-\rho_e S}(\rho_c(M)e^{-\tau/\mu_v} + \rho_e(M)t_d(\theta_v)) \quad (7)$$

If we now consider a patchy structure, we keep the same formalism as in Eq.(7), we only have to define a new environment reflectance noted $<\rho(M)>$ which represents a spatial average of each pixel reflectance over the whole surface.

$$\rho^*(\theta_s,\theta_v,\phi_s-\phi_v) = \rho_a(\theta_s,\theta_v,\phi_s-\phi_v) + \frac{T(\theta_s)}{1-<\rho(M)>S}(\rho_c(M)e^{-\tau/\mu_v} + <\rho(M)>t_d(\theta_v)) \quad (8)$$

This spatial average must be weighted by an atmospheric function which takes into account the efficiency of a point *M'* according to the distance from the point *M*, so $<\rho(M)>$ will be given by :

$$< \rho(M) >= \frac{1}{t_d(\theta_v)} \int_{-\infty}^{+\infty} \int_{-\infty}^{+\infty} \rho'(x,y)\ e(x,y,\theta_v)\ dx\ dy \qquad (9)$$

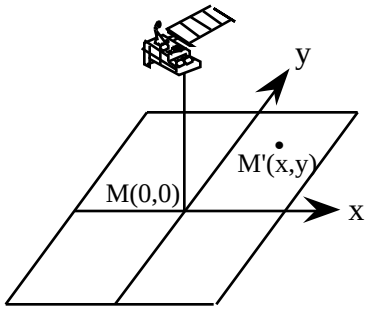

where

- *M* is the origin of the *x, y* coordinate system ;
- $\rho'(x,y)$ is the reflectance of the point *M'(x,y)* ;
- $e(x,y,\theta_V)$ is the contribution to the diffuse transmission $t_d(\theta_v)$ per unit area of an isotropic unit source placed at *M'(x,y)*.

The use of the same average reflectance $<\rho(M)>$ for the high orders of interaction (that is the geometrical series) is incorrect but reasonable because in most cases the contribution from these terms does not exceed 10-15% of the contribution of the first order term.

If we restrict the modeling to the case of vertical observations (or nearly, $\theta_v<30°$), Eq.(9) can be written

$$< \rho(M) >= \int_0^{2\Pi} \int_0^{\infty} \rho'(r,\phi) r p(r) dr\ d\phi \qquad (10)$$

with

$$r\ p(r) = \frac{re(r,\phi,0)}{t_d(0)} \qquad (11)$$

where (r,ϕ) are the polar coordinates of a given surface point with object pixel *M* at the origin. For off-nadir observation, we will see in the subroutine ENVIRO how to handle the problem.

Actually, it is impossible to solve this problem exactly, using Eq. (10) because of the computational time involved. Generally, we can define a characteristic size *r* of the target whose reflectance can be assumed uniform. By the same way, we can compute the environment reflectance ρ_e reflected by a simple arithmetical mean and we estimate $<\rho(M)>$ in the following manner.

Considers a circular target of radius r and reflectance ρ_C surrounded by homogeneous surface of reflectance ρ_e. Eq.(10) becomes :

$$< \rho(M) >= \rho_c F(r) + (1 - F(r))\rho_e \tag{12}$$

with

$$F(r) = 2\Pi \int_0^r r' p(r') dr' \tag{13}$$

which gives the relative contribution to $<\rho(M)>$ of surface points not farther than a distance r apart from the origin.

2.3 Intrinsic atmospheric reflectance

The intrinsic atmospheric reflectance observed over black target, $\rho_r+\rho_a$ is written here as the sum of aerosols and Rayleigh contributions. This decomposition is not valid at short wavelengths (less than $0.45\mu m$) or at large sun and view zenith angles.

2.3.1 Rayleigh

Atmospheric reflectance

For isotropic scattering, Chandrasekhar (1960) showed how solutions derived for small optical thicknesses may be extended to larger values of τ. He expressed the atmospheric reflectance $\rho^a(\mu_S,\mu_V,\phi_V-\phi_S)$ as

$$\rho_a(\mu_s, \mu_v, \phi_v - \phi_s) = \rho_a^1(\mu_s, \mu_v, \phi_v - \phi_s) + (1 - e^{-\tau/\mu_s})(1 - e^{-\tau/\mu_v})\Delta(\tau) \tag{14}$$

where $\rho_a^1(\mu_S, \mu_V, \phi_V - \phi_S)$ is the single-scattering contribution and the second term accounts roughly for higher orders of scattering.

In 6S, we use this approach to compute the molecular scattering reflectance.

Transmission function

The transmission function refers to the normalized flux measured at the surface. There are several approximate expressions based on the two-stream methods for computing the transmitted flux. The accuracy of these expressions depends on the scattering properties of the atmospheric layer (thick or thin clouds or aerosols) and on the geometrical conditions. The delta-Eddington method, which has been proved to be well suited for our conditions, has been selected. Since molecular scattering is conservative ($\omega_0=1$) and the anisotropy factor g is equal to zero, we may write

$$T(\mu) = \frac{[2/3 + \mu] + [2/3 - \mu]e^{-\tau/\mu}}{4/3 + \tau} \quad (15)$$

where μ is the cosine of the solar and/or observational zenith angle and τ is the optical thickness.

Spherical albedo

In conservative cases such as molecular scattering, the spherical albedo s is given by

$$s = 1 - \int_0^1 \mu\, T(\mu)\, d\mu \quad (16)$$

where $T(\mu)$ has been given in Eq.(15). Using Eqs.(15) and (16), the spherical albedo can be written as

$$s = \frac{1}{4 + 3\tau}\,[3\tau - 4\,E_3(\tau) + 6E_4(\tau)] \quad (17)$$

where $E_3(\tau)$ and $E_4(\tau)$ are exponential integrals for the argument τ.

2.3.2 aerosol

For the aerosols, the optical scattering parameters were computed using pre-defined models, Continental, Maritime, Urban or user's model based on a mixture of 4 basic components, Dust-Like, Oceanic, Water-Soluble, and Soot (provided by the World Climate Program). In 6S, these options are still usable but we added 2 news models, the Background Desertic Model and the Stratospheric model, and we also offer to the user the possibility of making up his own aerosol model (4 components maximum, see the description of the subroutine MIE for details).

In 5S, the scattering properties pertaining to the aerosol layer was performed using the Sobolev (1975) approximation for the reflectance, Zdunkowsky et al. (1980) for the transmittance and a semi-empirical formula for the spherical albedo. The reason was to provide the user having limited computing ressources with a fast approximation. The drawbacks to using these approximations were that the accuracy of the computations could be off by a few percent in reflectance units especially at large view and sun angles or high optical thicknesses. In addition, these approximations could be completely insufficient to handle the integration of the downward radiance field with non-lambertian ground conditions, a problem in simulating BRDF. The new scheme used to compute the aerosol+rayleigh coupled system relies on the Successive Orders of Scattering method. The accuracy of such a scheme is better than $1\ 10^{-4}$ in reflectance units. Other improvements on the 5S model include an atmosphere divided into 13 layers which enables exact simulations of airborne observations ; the downward radiation field is computed for a quadrature of 13 gaussian emerging angles which will provide the necessary inputs for BRDF simulations (see 2.5).

2.4 Airplane and elevated target simulations

2.4.1 Elevated target simulation

For a target not at sea level, Eq.(5) is modified as follows :

$$\rho^*(\theta_s,\theta_v,\phi_s-\phi_v,z_t) = Tg(\theta_s,\theta_v,z_t)\,[\rho_r(z_t)+\rho_a+\frac{\rho_t}{1-S(z_t)\,\rho_t}T(\theta_v,z_t)T(\theta_s,z_t)] \qquad (18)$$

The target altitude or pressure indicates the amount of scatterers above the target (molecules and aerosols) and the amount of gaseous absorbants. The target altitude z_t is handled in the following manner: After the atmospheric profile and the target altitude or pressure are selected, a new atmospheric profile is computed by stripping out the atmospheric level above target altitude and interpolating if necessary. This way, an exact computation of the atmospheric parameters are computed, without any kind of approximation which will account for coupled pressure-temperature effect on absorption.

Gaseous absorption

In most cases, only the integrated content may be modified. The user still has the option to enter the total amount of H_2O and O_3, but in this case the quantity entered must be representative of the level measured or estimated at the target location. The influence of target altitude on Tg has been evaluated. The absorption effect by O_3 is not sensitive to target altitude, because the ozone layer is located in the upper levels of the atmosphere, the variation of the altitude of the target does not modify this effect. The target's altitude has an important effect on the absorption by H_2O because most of the water vapor is located in the lower atmosphere. However the exact sensitivity of the target's altitude on water vapor absorption cannot be generalized because water vapor profile is variable.

Scattering function

The effect of target altitude on molecular optical thickness is accounted for in 6S. A good approximation, if needed, is to consider that τ_r is proportionnal to the pressure at target level. As the amount and types of aerosols are entered as parameters, the aerosol characteristics implicity depend on target altitude because measured at target location.

2.4.2 Airborne sensor simulation

In case of a sensor inside the atmosphere (aircraft simulation), Eq (5) is modified as following :

$$\rho^*(\theta_s,\theta_v,\phi_s-\phi_v,z) = Tg(\theta_s,\theta_v,z)\,[\rho_r(z)+\rho_a(z)+\frac{\rho_t}{1-S(z)\,\rho_t}\,T(\theta_v,z)T(\theta_s,z)] \qquad (19)$$

Gaseous absorption

Gaseous absorption is computed with a technique similar to the one used in the case of a target not at sea level. Only, the upward path is modified : the atmosphere level above the sensor altitude are stripped, so the computation is done only to the altitude of the sensor (interpolation of the atmospheric profile is conducted if necessary). The effect of altitude on gaseous transmission has been computed. For visible wavelength ranges, O_3 absorption on the target-sensor path is no longer accounted for due to the fact these molecules are located above most of aircraft sensors. H_2O absorption is very dependent on sensor altitude up to 4km. If the observed channel is sensitive to water vapor absorption (as it is in the case of AVHRR channel 2) we recommend that additionnal measurements of water vapor should be taken from the aircraft. An additional option has been set up in 6S for this purpose and enables the user to enter ozone and water vapor contents (as well as aerosol content) for the portion of the atmosphere located under the plane.

atmospheric reflectance and transmittance

In most cases the simple approximation "equivalent atmosphere", for atmospheric reflectance and transmittance is sufficiently accurate, ie :

$$\rho_r(z) \cong \rho_r(z=\infty,\tau_r(0\rightarrow z)) \qquad (20)$$

$$T(\tau_r,\theta_v,z) \cong T(\tau_r(0\rightarrow z),\theta_v,z=\infty) \qquad (21)$$

which means that computations are performed for optical thicknesses corresponding to the integration between the surface and the sensors.

In 6S, the computation is performed exactly by defining one of the multiple layers used in the Successive Orders of Scattering as the altitude of the sensor. This enables exact computation of both reflectance and transmission term for a realistic mixing between aerosol and Rayleigh.

2.4.3 Non uniform target

In 5S, the case of a non-homogeneous target is solved using Eqs.(8) and (12) where the function F(r) is defined as

$$F(r) = \frac{t_d^r(\mu_v)F^r(r) + t_d^a(\mu_v)F^a(r)}{t_d(\mu_v)} \qquad (22)$$

The problem of a target not at sea level, as long as we consider that the target and environment are at the same altitude, can be solved just by modifying the Rayleigh optical thickness.

In the case of aircraft observations, first we have to take into account the reduction of the amount of scatterers under the plane. This can be done just by adjusting $t_d^r(\mu_v)$ and $t_d^a(\mu_v)$ to $t_d^r(z,\mu_v)$ and $t_d^a(z,\mu_v)$. Once this has been done, the principal part of the effect accounted for is a global reduction (factor 5-10 for an altitude of flight of 6 km) of the "environment effect". The second effect is the dependence of $F^r(r)$ and $F^a(r)$ upon altitude of the sensor. Monte Carlo simulation of $F^r(r)$ and $F^a(r)$ have been performed for different altitudes of the sensor (0.5,....12km) and included in 6S as a database. In case of a plane observation, the closest simulated altitudes are used to interpolate the environment function at the aircraft altitude.

2.5 Directional effect of the target

2.5.1. BRDF

In 6S, the coupling of BRDF with the atmosphere is addressed, the contribution of the target to the signal at the top of the atmosphere is decomposed as the sum of four terms :

• the photons directly transmitted from the sun to the target and directly reflected back to the sensor

$$e^{-\tau/\mu_s}\rho_t(\mu_s,\mu_v,\phi)e^{-\tau/\mu_v} \tag{23}$$

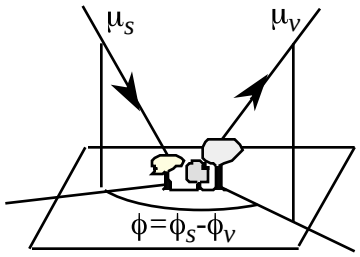

• the photons scattered by the atmosphere then reflected by the target and directly transmitted to the sensor,

$$t_d(\mu_s)\,\bar{\rho}_t(\mu_s,\mu_v,\phi)\,e^{-\tau/\mu_v} = t_d(\mu_s)\frac{\int_0^{2\pi}\int_0^1 \mu\, L^{\downarrow}(\mu_s,\mu,\phi')\,\rho_t(\mu,\mu_v,\phi'-\phi)\,d\mu\,d\phi'}{\int_0^{2\pi}\int_0^1 \mu\, L^{\downarrow}(\mu_s,\mu,\phi')\,d\mu\,d\phi'}\,e^{-\tau/\mu_v} \tag{24}$$

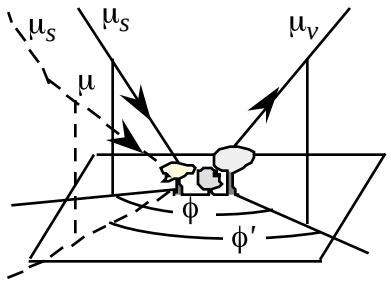

• the photons directly transmited to the target but scattered by the atmosphere on their way to the sensor,

$$t_d(\mu_v)\,\overline{\rho}_t'(\mu_s,\mu_v,\phi)\,e^{-\tau/\mu_s} = t_d(\mu_v)\,\overline{\rho}_t(\mu_v,\mu_s,\phi)\,e^{-\tau/\mu_s} \qquad (25)$$

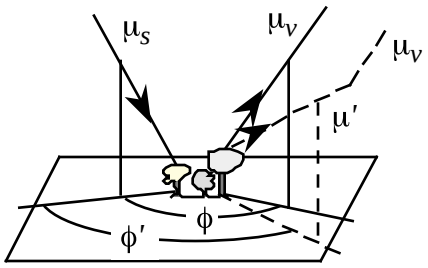

• the photons having at least two interactions with the atmosphere and one with the target :

$$t_d(\mu_v)\,t_d(\mu_s)\,\overline{\overline{\rho}}_t + \frac{T_{R+A}(\mu_s)\,T_{R+A}(\mu_v)\,S\left(\overline{\rho}_t\right)^2}{1-S\overline{\rho}_t} \qquad (26)$$

with $\overline{\overline{\rho}}_t = \overline{\overline{\rho}_t'(\mu_s,\mu_v,\phi)}$

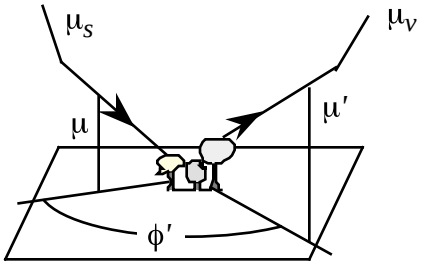

In 6S, the first three contributions are computed exactly using the downward radiation field as given by the Successive Orders of Scattering method. The contribution which involves at least two

interactions between the atmosphere and the BRDF (Eq.(26)) is approximated by taking $\overline{\overline{\rho}}_t$ equal to the the hemispherical albedo of the target

$$\overline{\overline{\rho}}_t \cong \int_0^1 \mu_s \int_0^{2\pi} \int_0^1 \mu \, \rho_t(\mu_s,\mu_v,\phi'-\phi) \, d\mu_v \, d\phi \, d\mu_s \tag{27}$$

This approximation is required because the exact computation needs a double integration which would result in very long computation times. It is in addition justified by the limited impact on the total signal of this last contribution mitigated by $t_d(\mu_S)\, t_d(\mu_V)$ and also because the radiation field after one interaction trends to be isotropic.

2.5.2. Sunglint

The solar radiation directly reflected by the water surface is computed exactly with the Snell-Fresnel laws. For a rough sea surface, the reflection is conditioned by the wind and its description is by necessity a statistical one. Thus, the model surface can be computed numerically by many facets whose slopes are described by a Gaussian distribution (Cox and Munk, 1954). In 6S, this slope distribution is considered anisotropic (depending upon wind direction). Operationally, the scheme to compute the reflection by the sunglint is identical to BRDF ones.

2.6 Atmospheric correction scheme.

An input parameter allows to activate atmospheric correction mode. In this case, the ground is considered to be Lambertian , and as the atmospheric condition are known the code retrieves the atmospherically corrected reflectance value ρ_{ac} that will produce the reflectance (or the radiance) equal to the apparent reflectance ρ_i^* (Eq. (1)) (or apparent radiance) entered as input. Following Eq. 5, ρ_{ac} be determined as :

$$\rho_{ac}(\theta_s,\theta_v,\phi_s-\phi_v) = \frac{\rho'_{ac}}{1+\rho'_{ac}\, s} \tag{28}$$

with

$$\rho'_{ac} = \frac{\dfrac{\rho_i^*(\theta_s,\theta_v,\phi_s-\phi_v)}{Tg} - \rho_a(\theta_s,\theta_v,\phi_s-\phi_v)}{T(\theta_s)\, T(\theta_v)} \tag{29}$$

where ρ_i^* is the input parameter and where all the others parameters are computed in the atmospheric conditions described by the user.

3 *Interaction between absorption and scattering effects*

The atmospheric radiation depends on atmospheric transmittances which can be modified by the contribution of absorbing gases. The gaseous absorption must therefore be computed for each scattering path. We can simplify the problem and separate the two processes.

Let us consider the O_3 gas. It is localized at altitudes where molecules and aerosols are sparse, then the incident and reflected radiation go through the O_3 layer nearly without scattering. So, we compute the atmospheric radiation ρ^* without accounting for O_3. We modify the signal by the only direct transmittance which corresponds to the twofold paths :

$$Tg_{O_3}(\theta_s, \theta_v, U_{O_3}) \tag{30}$$

where U_{O_3} is the absorber amount.

In the case of H_2O and CO_2, the absorption bands occur in the near and middle infrared. In this range, the molecular scattering becomes negligible and we only have to take into account the aerosol scattering. Some simulations, made for realistic atmospheres, show that beyond 0.850μm, the 1st and 2nd scattering constitute almost the whole diffuse radiation. Because the aerosol phase function has a large forward scattering, the diffuse paths are not completely separate from direct paths and we shall consider that the influence of CO_2 or H_2O upon scattered flux is the same as for direct solar flux. So the diffuse and transmitted flux will be both reduced by the factor

$$Tg_{H_2O}(\theta_s, \theta_v, U_{H_2O}) Tg_{CO_2}(\theta_s, \theta_v, U_{CO_2}) \tag{31}$$

For O_2, the absorption is very localized and presents a very narrow band, so we take into account this gas by the same way :

$$Tg_{O_2}(\theta_s, \theta_v, U_{O_2}) \tag{32}$$

We have checked our approximation from a simulation in the visible Meteosat spectral band. This band is large enough (0.35-1.10μ*m*) to include both scattering effects and water vapor absorption. To amplify the coupling effect, we have taken a tropical atmosphere model (H_2O content is about $4 g/cm^2$) and a continental aerosol model with large optical depth ($\tau_{0.55\mu m}$ =1). For $\Delta\nu$=20cm^{-1}, we have :

μ_s	$T^{exact}(\theta_S)$	$T^{est}(\theta_S)$
1.0	*0.837*	*0.843*
0.5	*0.692*	*0.693*
0.1	*0.401*	*0.363*

Estimation of the accuracy of our approximation

The comparison between exact computations and results obtained from our approach is reported in the above table for three solar angles. Except for a grazing incidence (μ_s=0.1), we have a good agreement and the error related to this approximation is smaller than one percent.

For atmospheric reflectance, the problem is slightly different. The diffuse paths are not close to the direct paths. The photons are scattered at large angles away from the forward direction. For O_3, the same approximation is still justified because it is based upon the weak interaction between the two processes. For H_2O, the scale height is comparable to the aerosols scale height while CO_2 is uniformly mixed. Therefore, for these two gases our approximation is less valid but remains sufficiently accurate as long as the gaseous absorption is small, i.e. in the atmospheric windows.

For getting the maximum uncertainties resulting from the approximation, we consider 3 extreme cases in 6S: the water vapor above the aerosol layer (maximum absorption, see (33-a) for i=3), the water vapor under the aerosol layer (minimum absorption, see (33-a) for i=1), and an average case where we consider that half of the water vapor present in the atmosphere absorbs the aerosol path radiance (see (33-a) for i=2). In that respect, the satellite signal is written

$$\rho_{TOA}^{i=1,3}(\theta_s,\theta_v,\phi_s-\phi_v) = Tg^{OG}(\theta_s,\theta_v)\,[\rho_R + (\rho_{R+A}-\rho_R)Tg^{H_2O}(\theta_s,\theta_v,\tfrac{i-1}{2}U_{H_2O})$$

$$+ T^{\downarrow}(\theta_s)\,T^{\uparrow}(\theta_v)\,\frac{\rho_s}{1-S\,\rho_s}\,Tg^{H_2O}(\theta_s,\theta_v,U_{H_2O})\,] \qquad (33\text{-}a)$$

where Tg^{OG} refers to the gaseous transmission for other gases than water vapor, Tg^{H_2O} refers to H_2O absorption and ρ_{R+A}-ρ_R is an estimate of the aerosol intrinsic reflectance. For each cases, we compute the top of the atmosphere reflectance, so the uncertainty due to the vertical distribtution of aerosol versus water vapor can be considered.Tg^{OG} is computed on the sun-target-satellite direct paths using

$$Tg^{OG}(\theta_s,\theta_v) = \prod_{i=1}^{8} Tg_i(\theta_s,\theta_v,U_i) \qquad (33\text{–}b)$$

CONCLUSION

An accurate analytical expression of the reflectance measured by a satellite-sensor or by a sensor aboard an aircraft has been established.

- In the case of Lambertian and uniform surface, we completely separate the surface-atmosphere system and define three atmospheric functions.
  - the intrinsic atmospheric signal component
  - the total transmittance
  - the spherical albedo.

- The coupled BRDF-atmosphere are accounted for according to the same scheme by definition of mean angular reflectances which are depending on atmospheric properties.

- In the case of a non-uniform ground, we have defined a spatial average reflectance which remains slightly dependent on atmospheric properties by the definition of the function *F(r)*. This function allows us to take into account the main blurring atmospheric effect for non-uniform surfaces.

- In both cases, it is possible to consider elevated targets.

The absorption by atmospheric gases is computed separately as a simple multiplicative factor. The solar spectrum is divided into spectral intervals of $10 cm^{-1}$ width.

In addition, a scheme of atmospheric correction is available.

The computational aspect of our work is now detailed in the following appendix:

- Appendix I : General description of the computer code
- Appendix II : Example of inputs and outputs
- Appendix III : Complete description of the subroutines

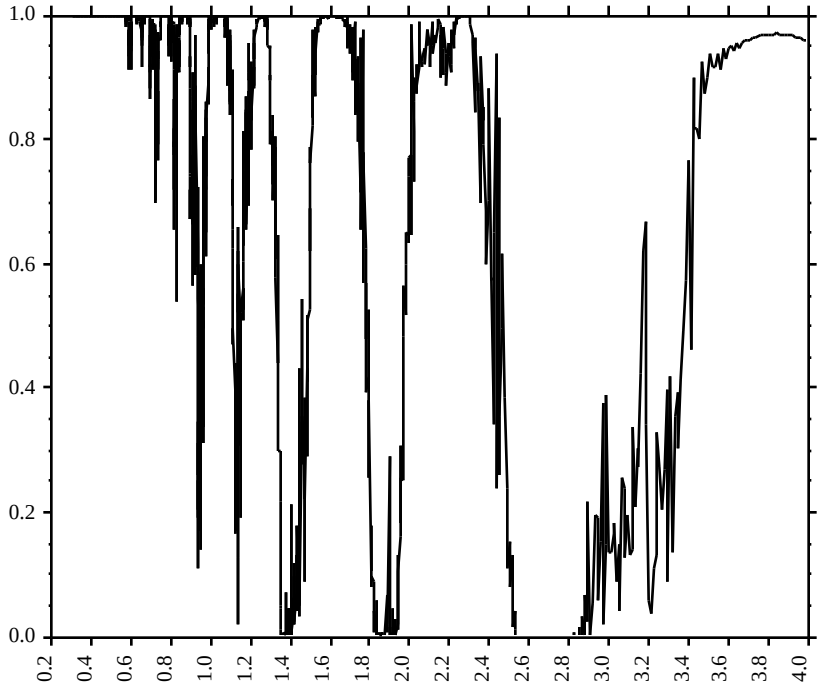

Fig. I-1: Spectral transmittance of H_2O

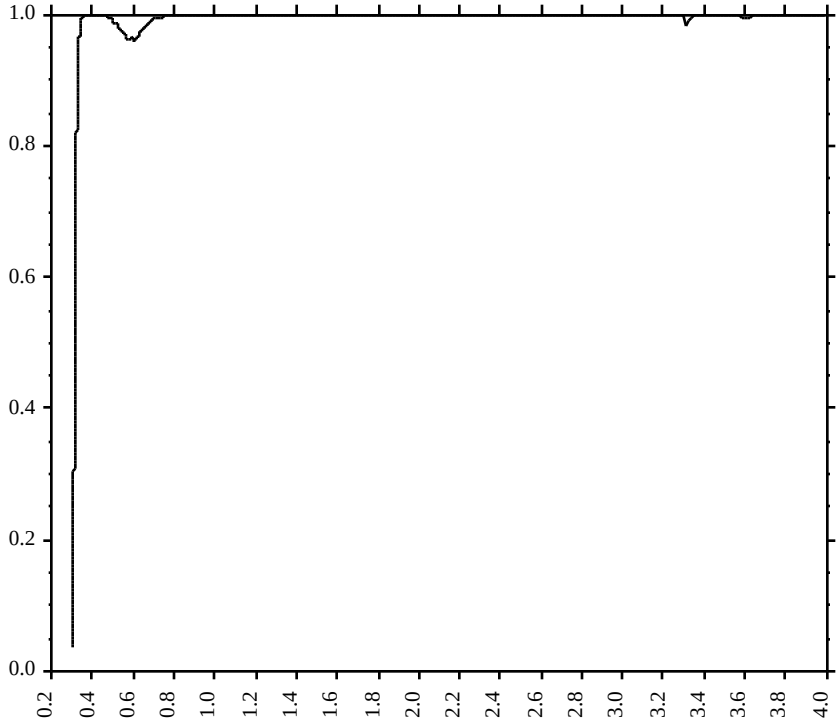

Fig. I-2: Spectral transmittance of O_3

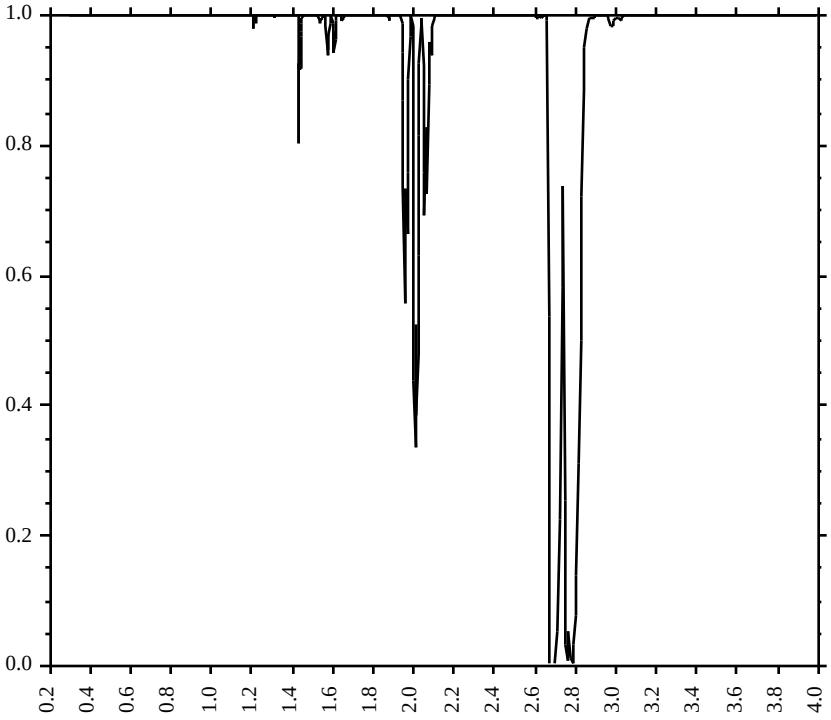

Fig. I-3: Spectral transmittance of CO_2

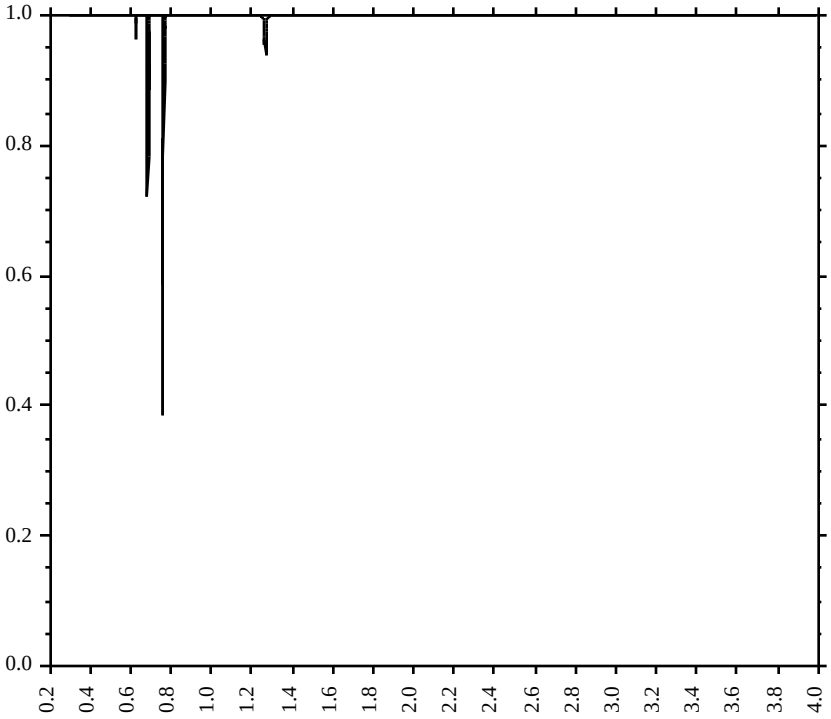

Fig. I-4: Spectral transmittance of O_2

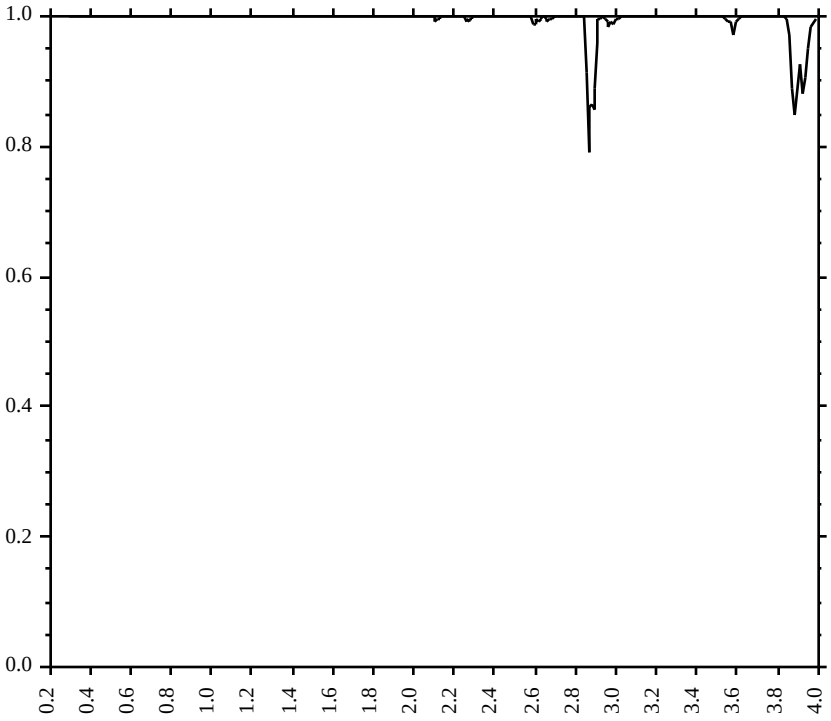

Fig. I-5: Spectral transmittance of N_2O

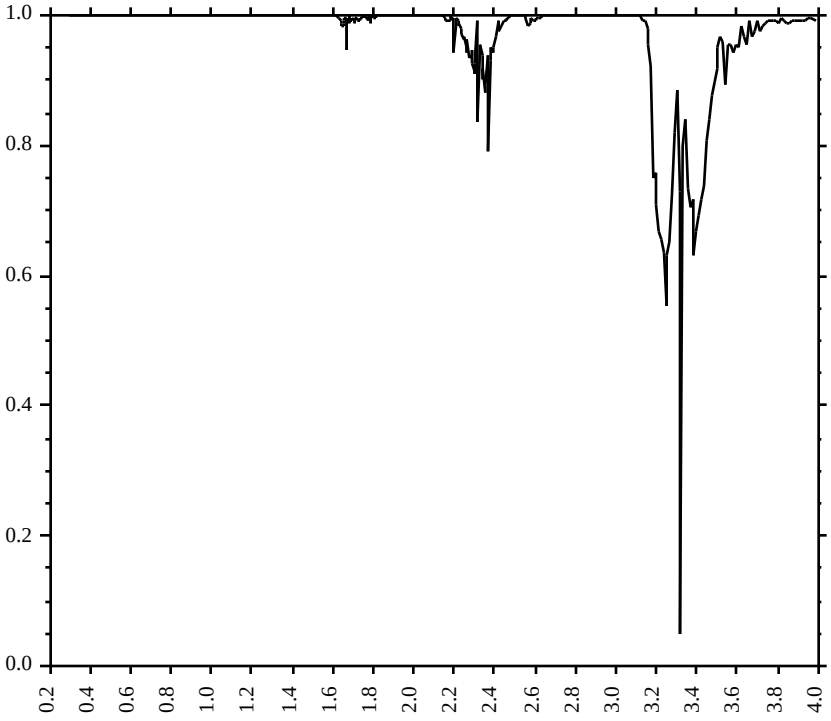

Fig. I-6: Spectral transmittance of CH_4

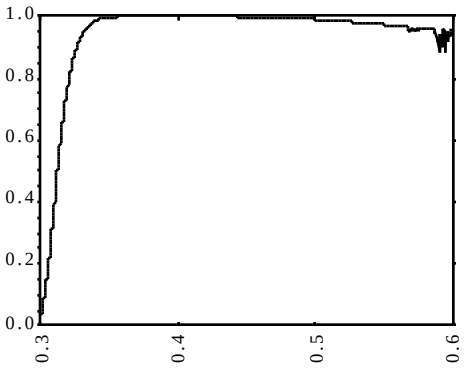

Fig. I-7: Atmospheric window at 0.40μ*m*

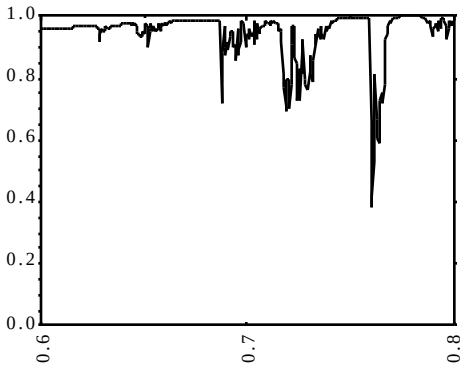

Fig. I-8: Atmospheric window at 0.75μ*m*

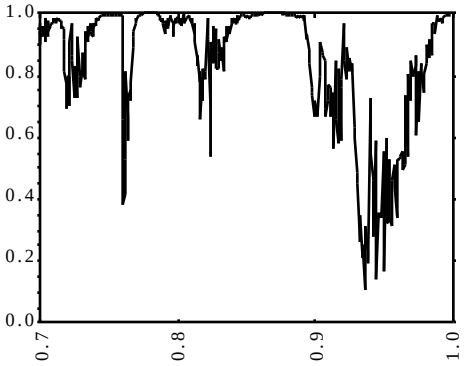

Fig. I-9: Atmospheric window at 0.85μ*m*

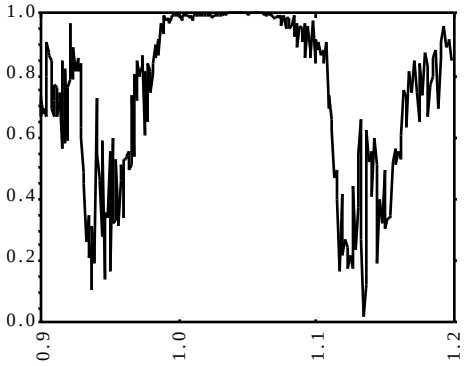

Fig. I-10: Atmospheric window at 1.06μ*m*

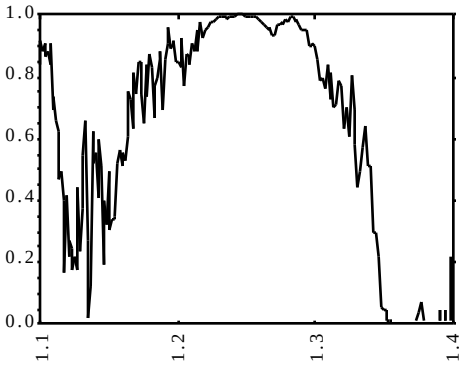

Fig. I-11: Atmospheric window at 1.22μ*m*

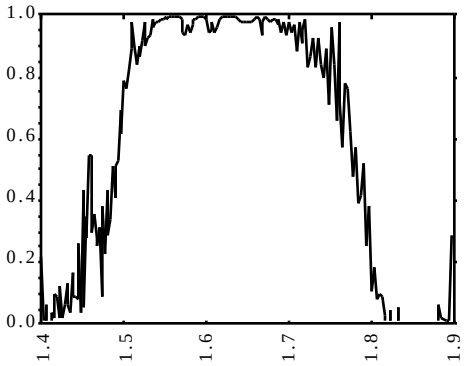

Fig. I-12: Atmospheric window at 1.60μ*m*

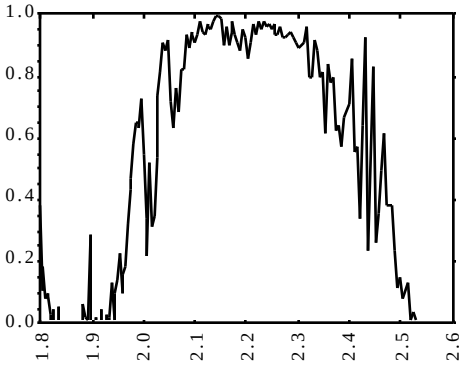

Fig. I-13: Atmospheric window at 2.20μ*m*

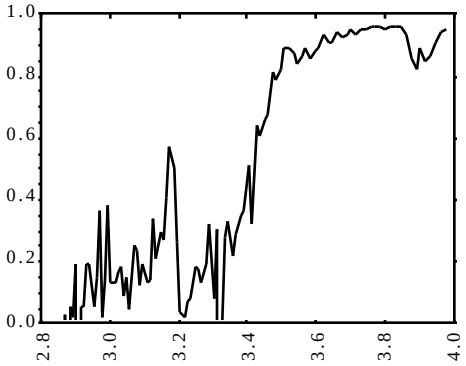

Fig. I-14: Atmospheric window at 3.70μ*m*

ACKNOWLEDGEMENTS

The authors would like to thank Nazmi El Saleous from the GIMMS group for his help in putting together this manual, Lorraine Remer from Code 923 for having kindly read the first draft of this manual and help us to improve it. They are very grateful to Dr. Tucker and Justice from GSFC/UMD for the logistic support essential to the realization of 6S. Finally, special thanks to all the Beta tester of the code and in particular to Phil Teillet from Canadian Centre for Remote Sensing for his interesting and useful remarks. The Laboratoire d'Optique Atmosphérique is sponsored by CNRS (Centre National de Recherche Scientifique) and by CNES (Centre National d'Etudes Spatiales).

APPENDIX I: DESCRIPTION OF THE COMPUTER CODE

This code predicts the satellite signal between 0.25 and 4.0 μm assuming cloudless atmosphere. Let us recall that the apparent reflectance at the satellite level for Lambertian surface can be written,

$$\rho'(\theta_s,\theta_v,\phi_v) = t_g(\theta_s,\theta_v)\{\rho_a(\theta_s,\theta_v,\phi_v) + \frac{T(\theta_s)}{1- <\rho(M)> S}[\rho_c(M)e^{-\tau/\mu_v} + <\rho(M)> t_d(\theta_v)]\}$$

This formalism takes into account the main atmospheric effects, gaseous absorption by H_2O, O_2, CO_2 and O_3, scattering by molecules and aerosols and a non-homogeneous ground may be considered. The general flow chart for 6S program is reported in Figure A-1

The following input parameters are necessary:

- geometrical conditions,
- atmospheric model for gaseous components,
- aerosol model (type and concentration),
- spectral condition,
- ground reflectance (type and spectral variation).

At each step, you can either select some proposed standard conditions or define your own conditions. More details are given in Figures A-2 to A-9. Let us note that the satellite navigation is done by a rough calculation from the nominal characteristics of the satellite orbit. It is obvious that, without anchor points, the localization is not very accurate.

From these data, we compute the scattering atmospheric functions, at ten wavelengths which are well distributed over the solar spectrum (Fig. A-11). At any wavelength, we interpolate from these values by assuming the spectral dependance

$$f(\lambda) = f(\lambda_0)\left(\frac{\lambda}{\lambda_0}\right)^{-\alpha}$$

and compute the apparent reflectance from the first equation (Fig.A-10)

We have reported on Fig. A-12 the general outputs and the optional ones.

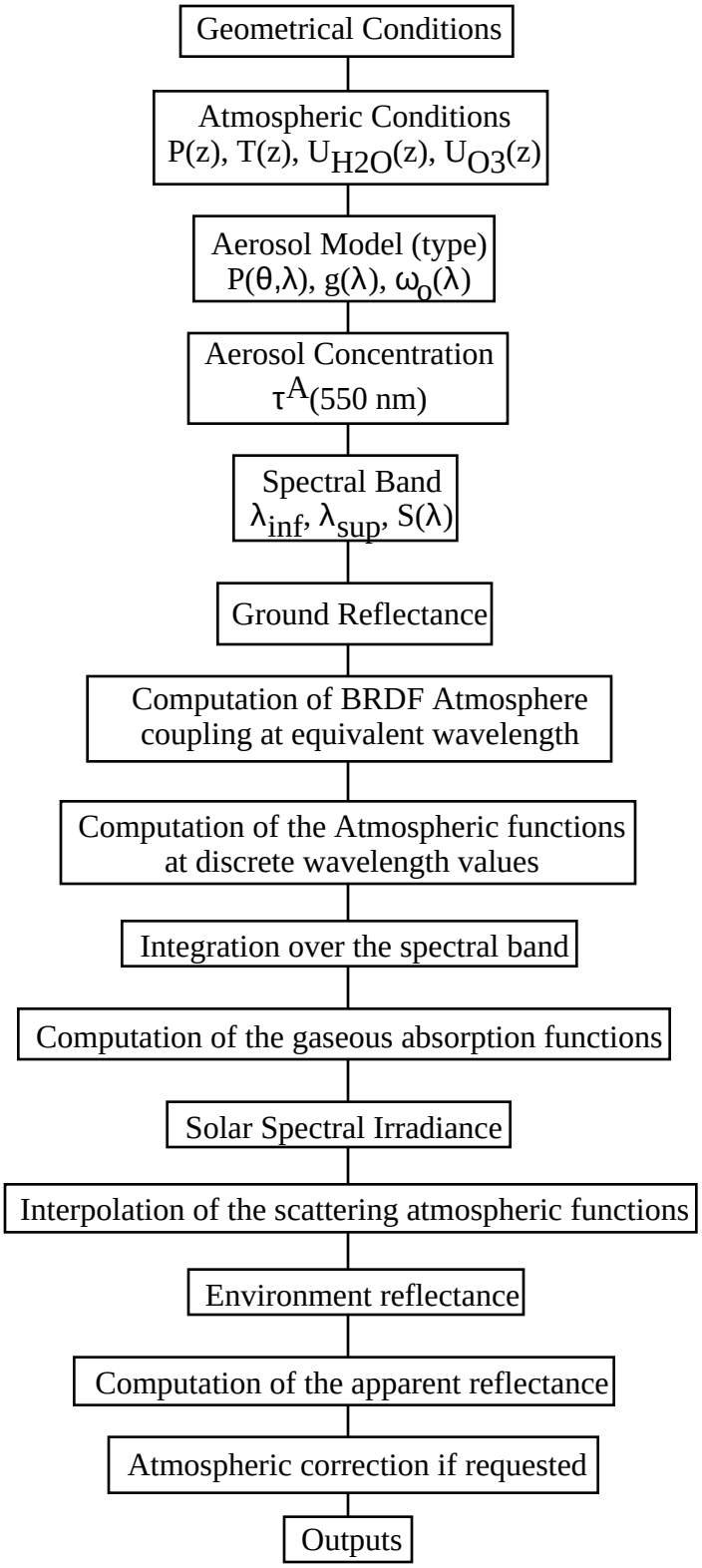

Figure A-1 : General flow chart 6S computations

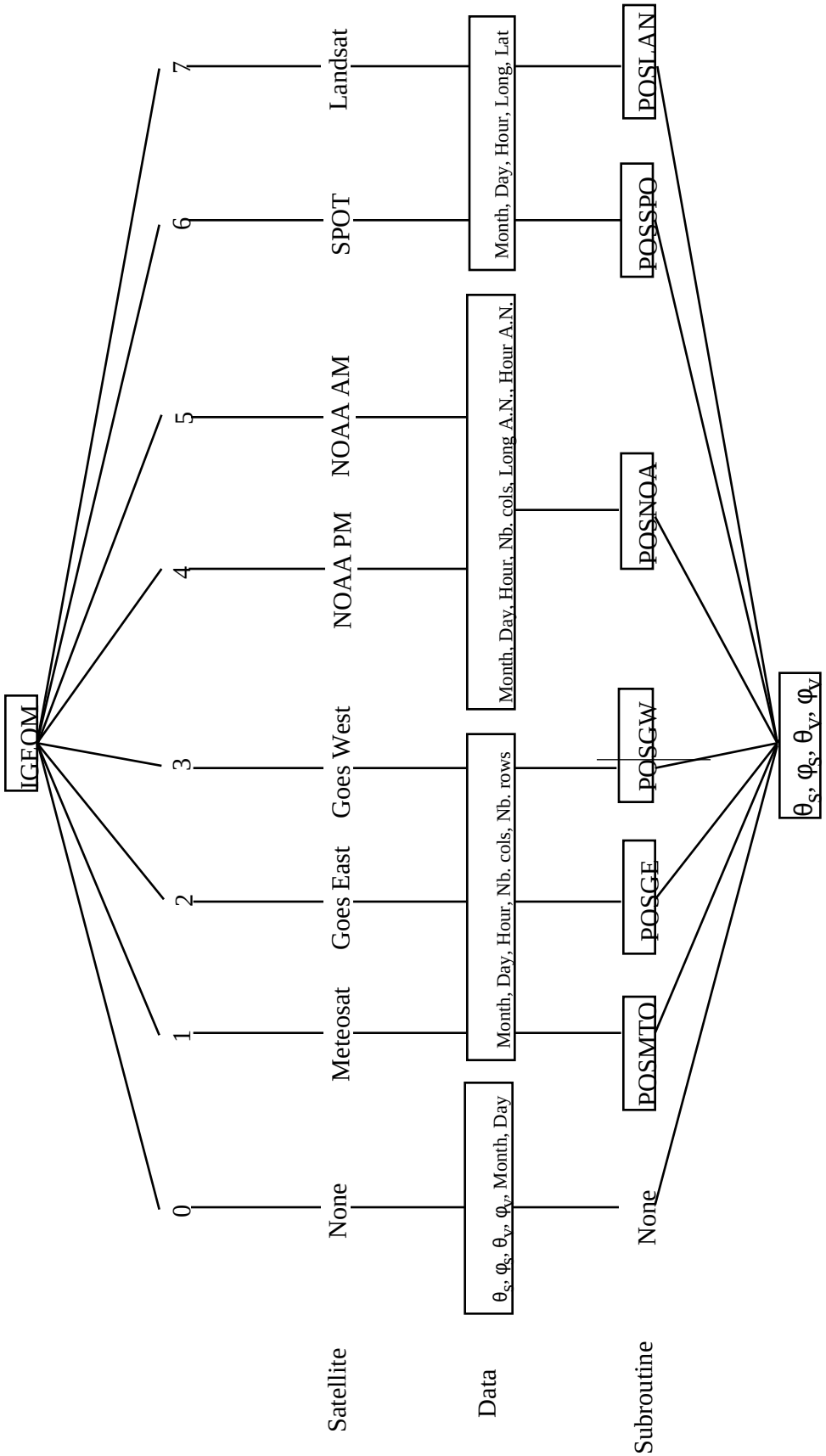

Figure A-2

: Detailed Flow Chart for Geometrical Conditions

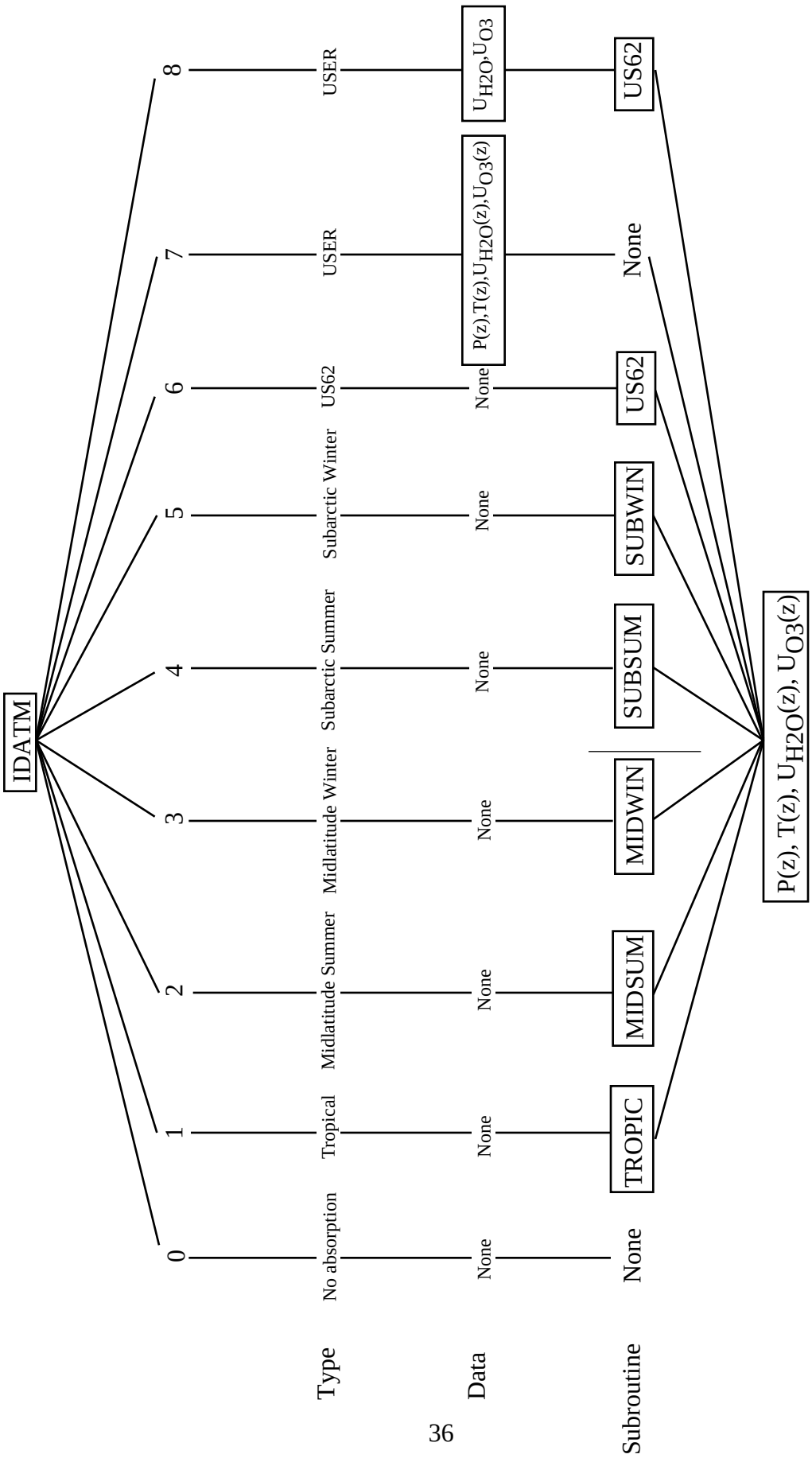

Figure A-3

: Detailed Flow Chart for Atmospheric Conditions

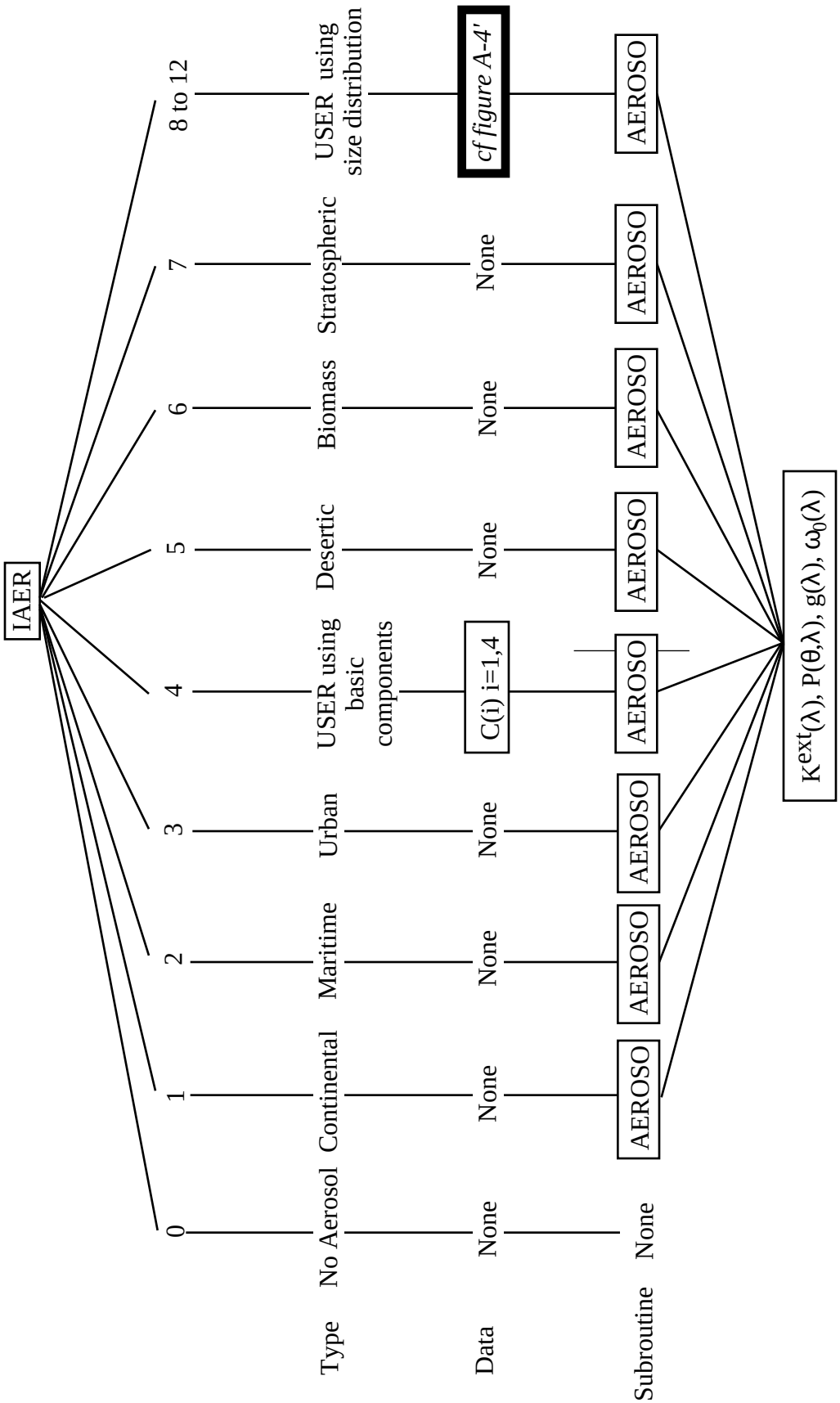

Figure A-4

: Detailed Flow Chart for Aerosol Model (Type)

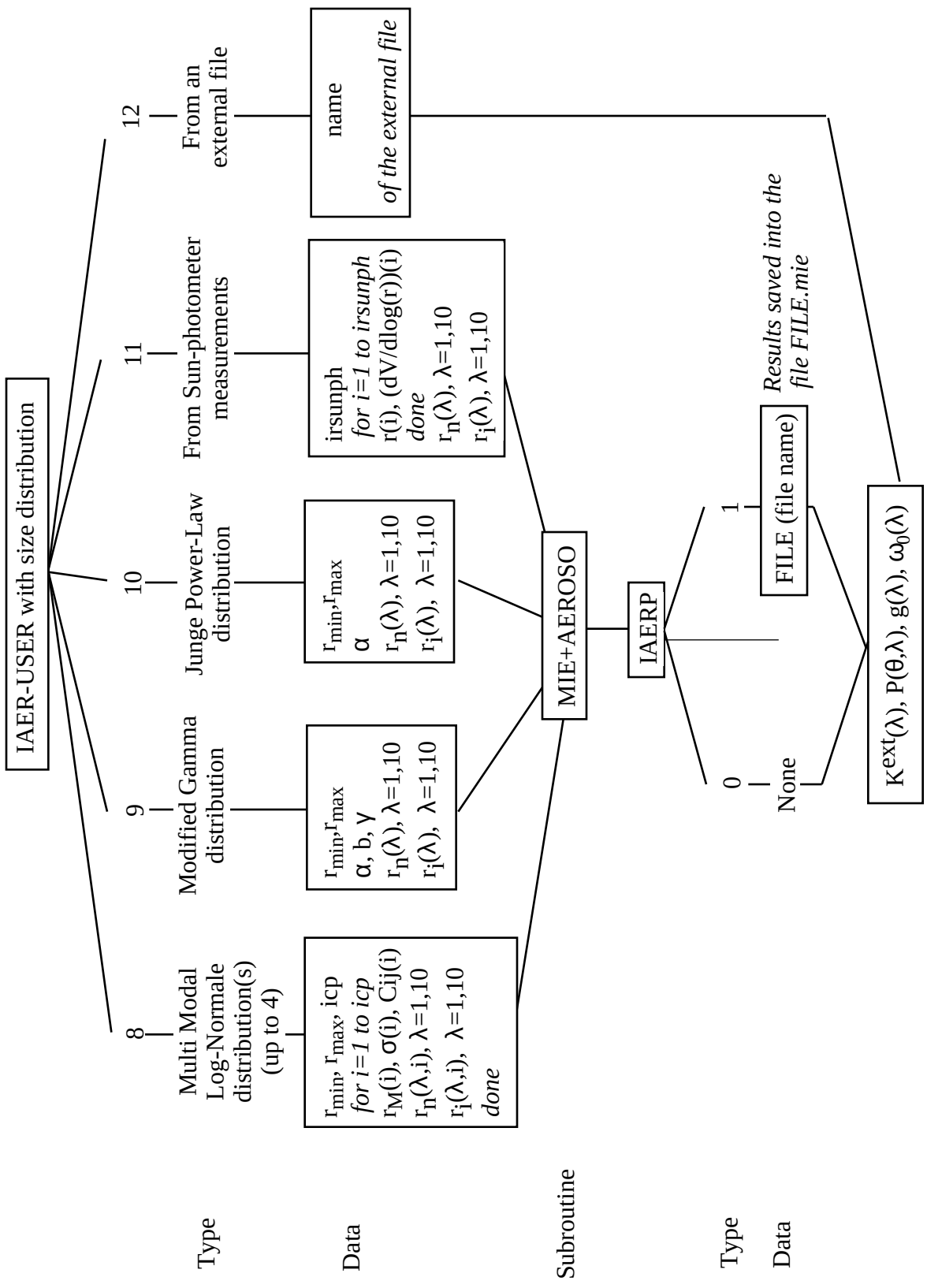

Figure A-4'

: Detailed Flow Chart for Aerosol Model (Type)

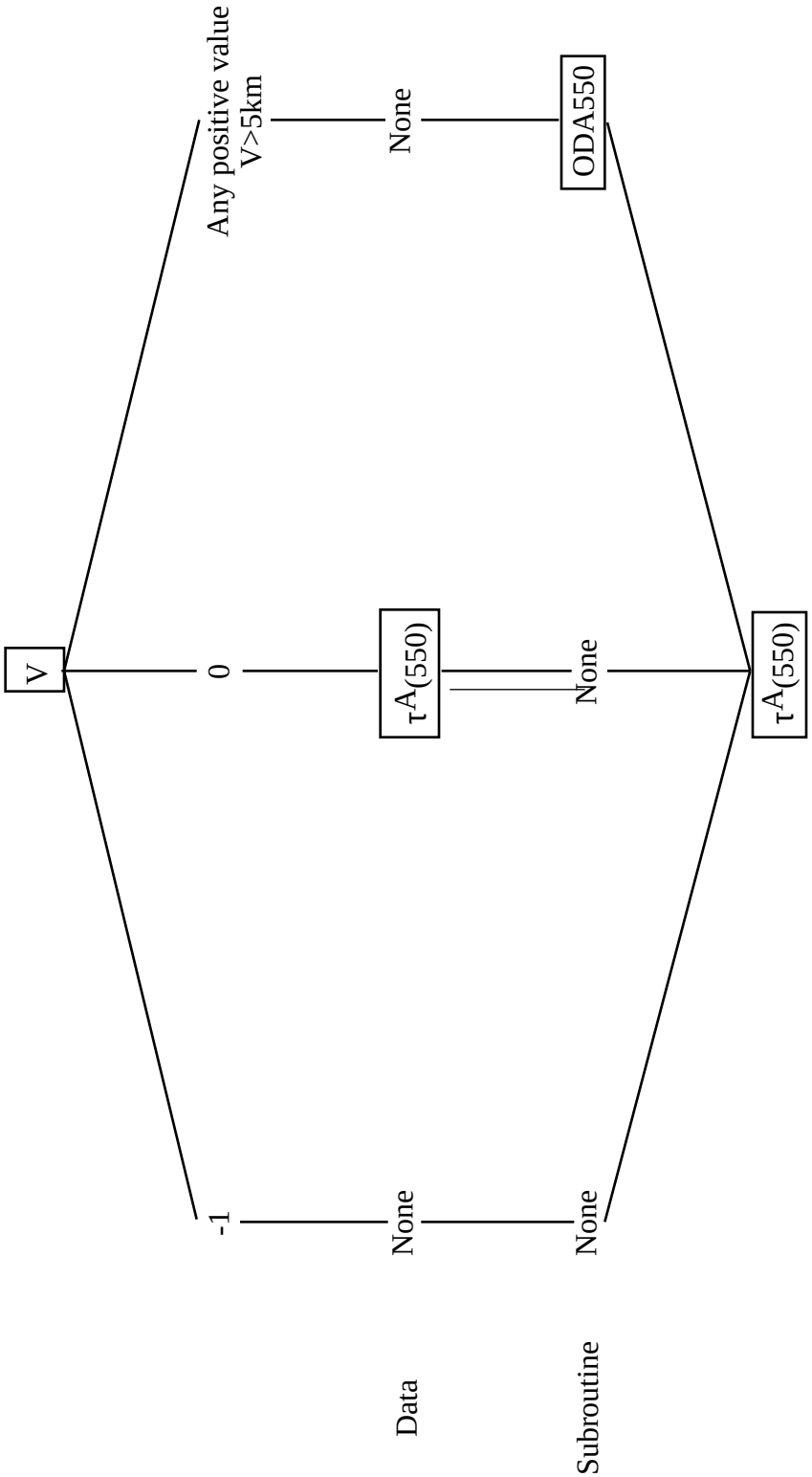

Figure A-5

: Detailed Flow Chart for Aerosol Model (Concentration, $\tau^A(550)$)

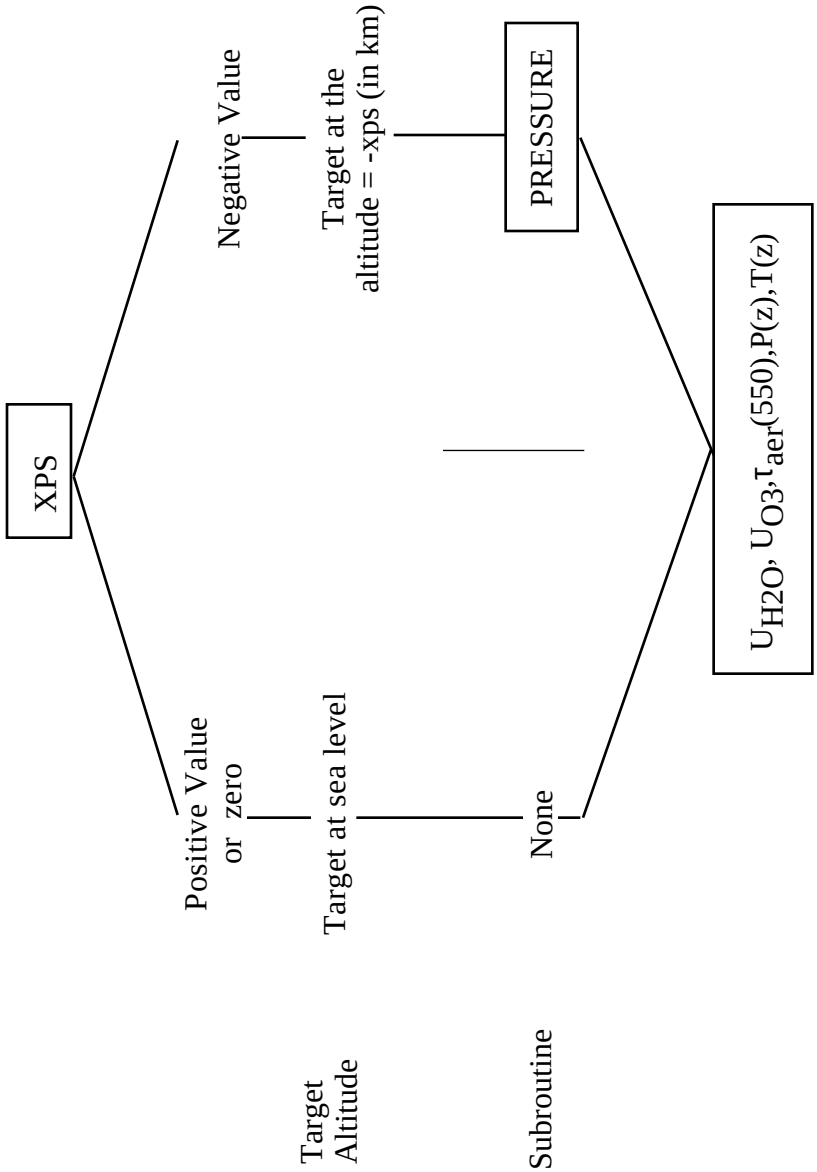

Figure A-6

: Detailed Flow Chart for the effect of the altitude: Target

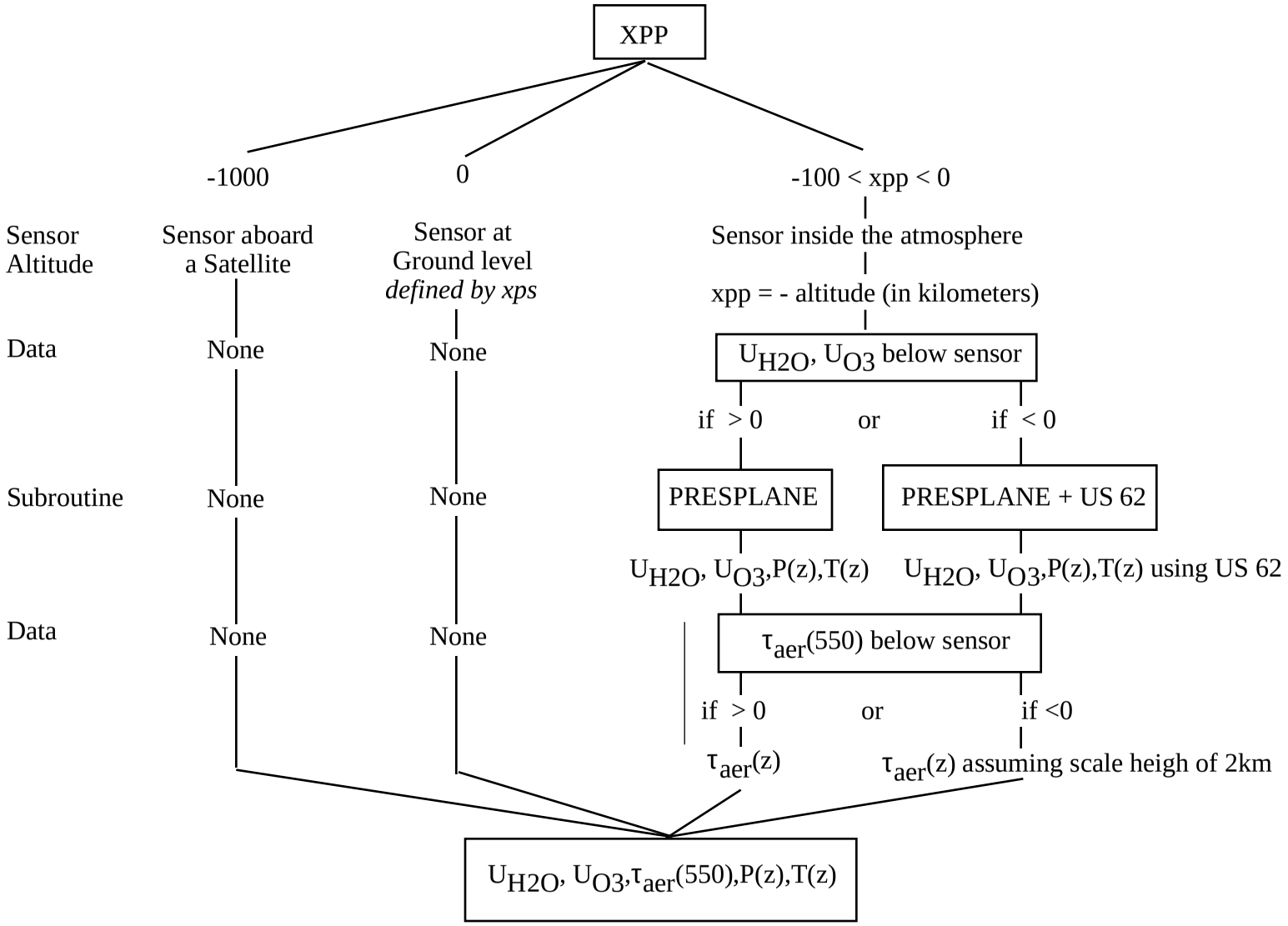

Figure A-6'

: Detailed Flow Chart for the effect of the altitude: Sensor

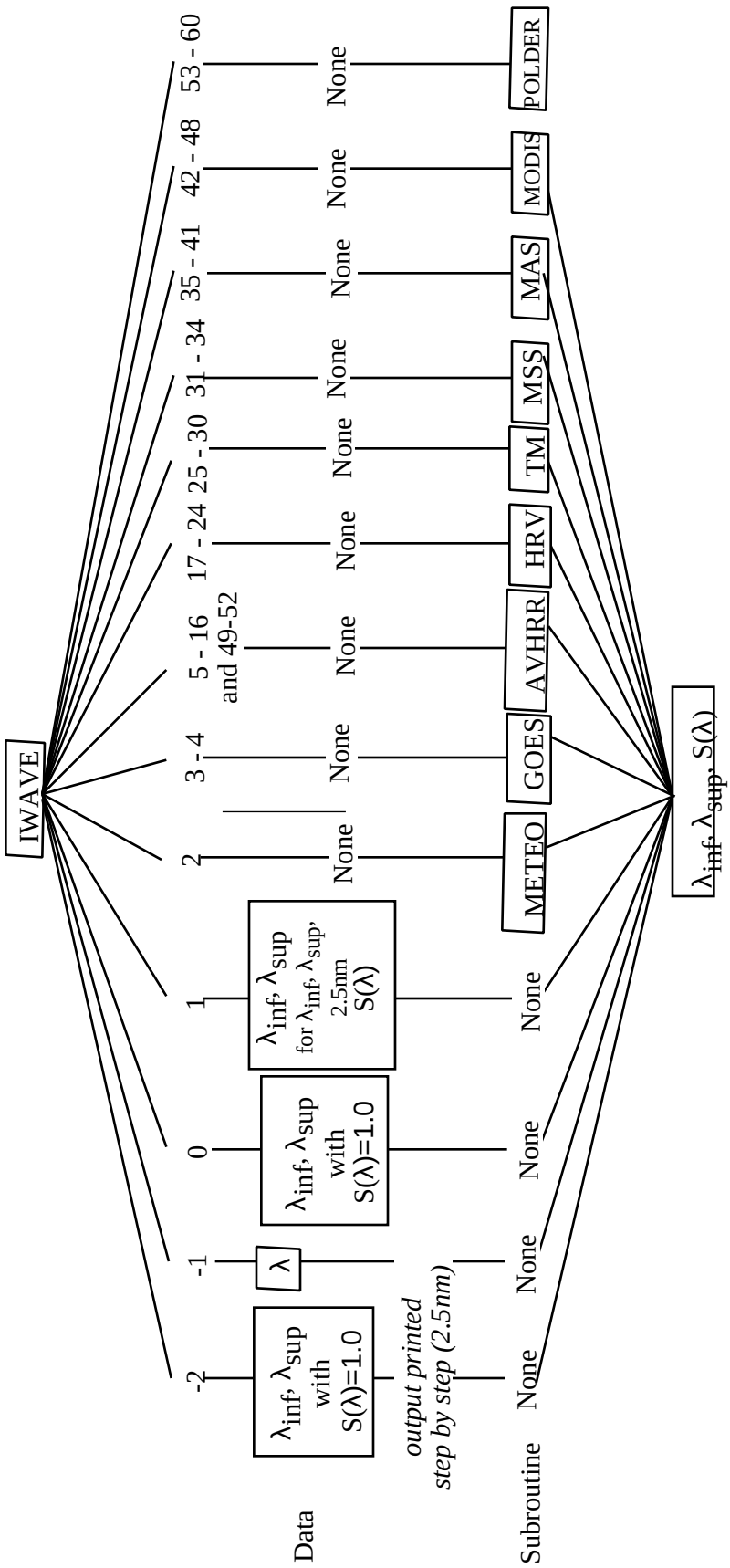

Figure A-7

: Detailed Flow Chart for Spectral Band Definition of Extreme Wavelengths and Filter Function

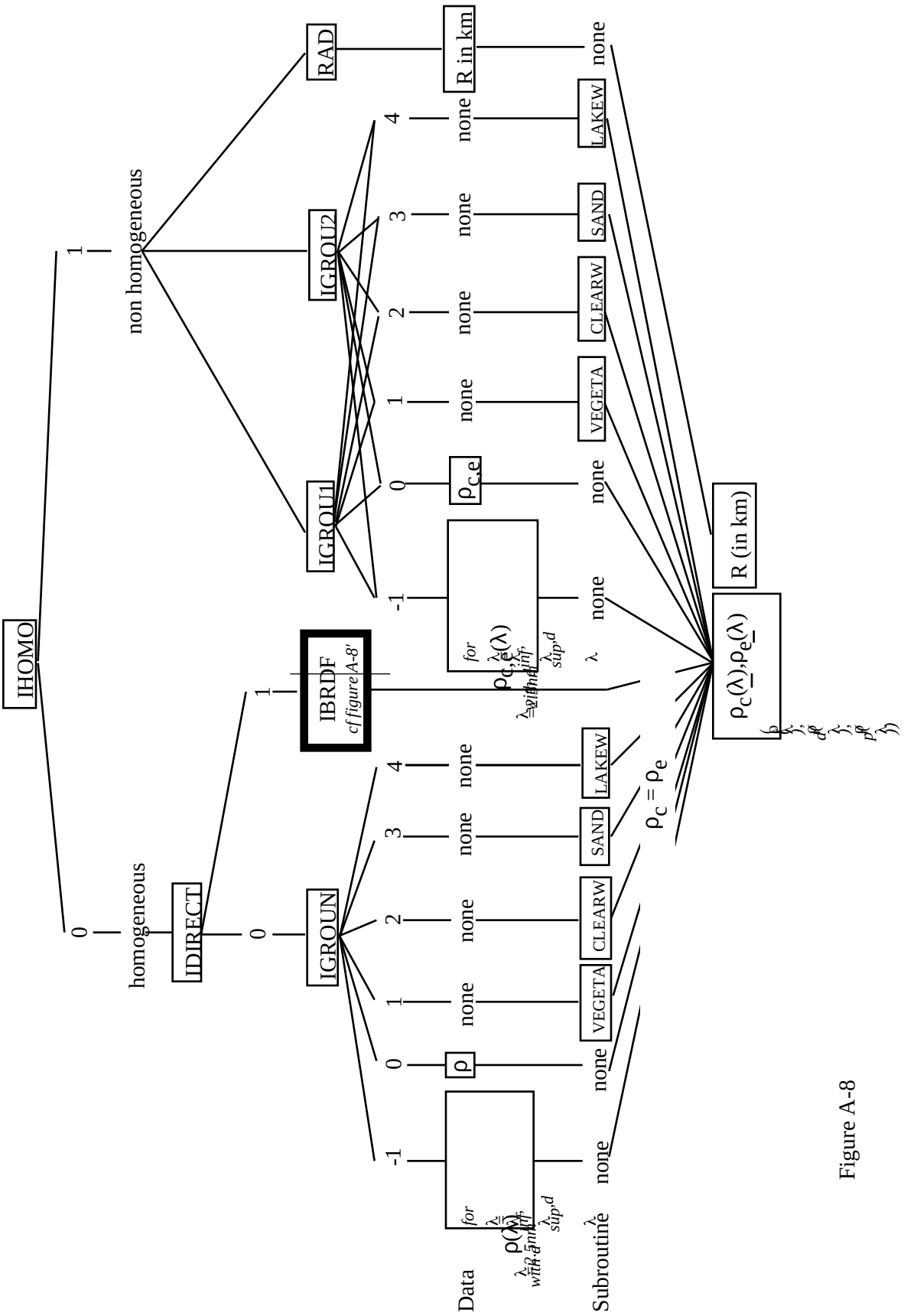

Figure A-8

: Detailed Flow Chart for Ground Reflectance, Definition of the Target and Environment Reflectances

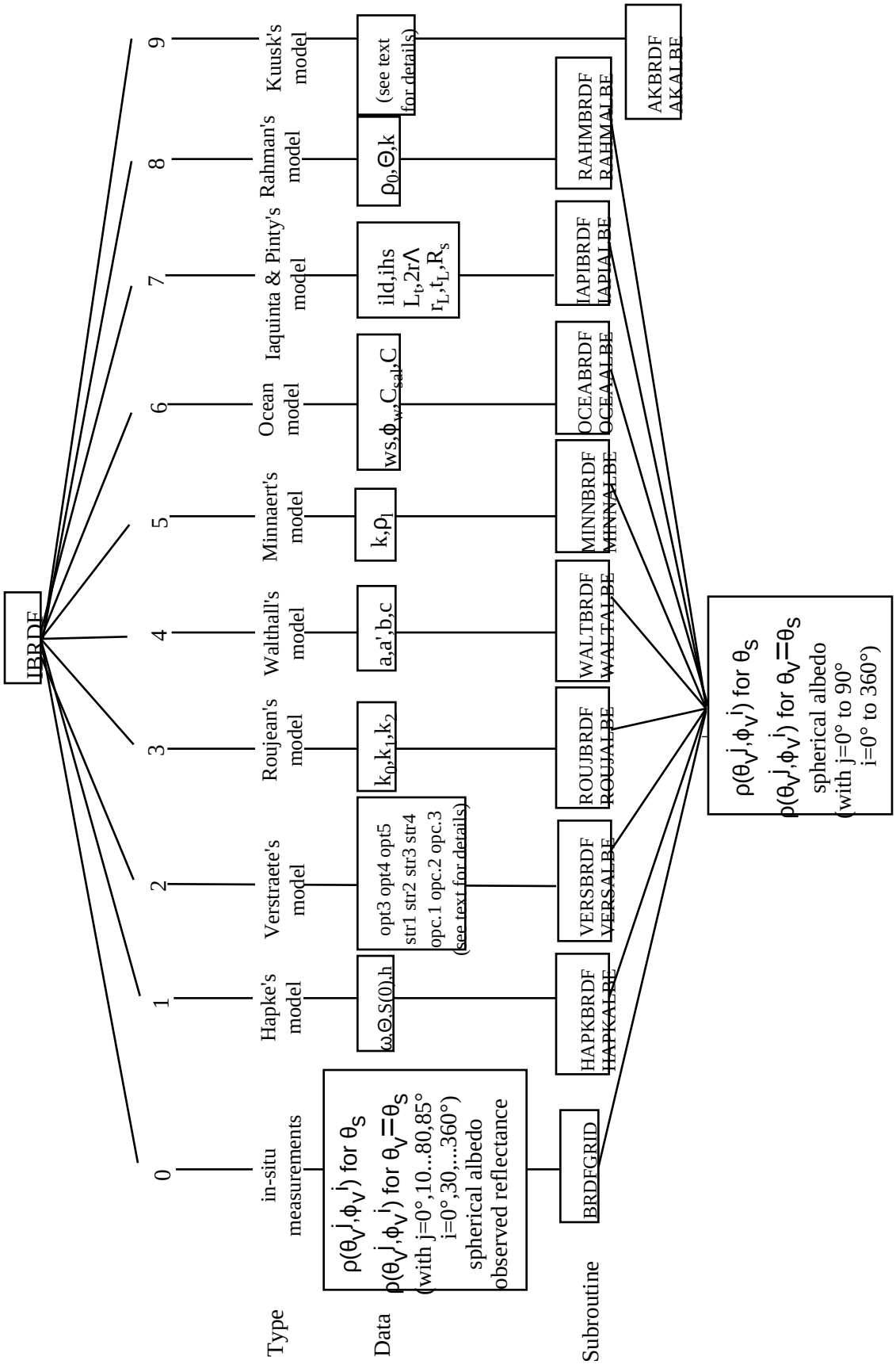

Figure A-8' : Detailed Flow Chart for BRDF

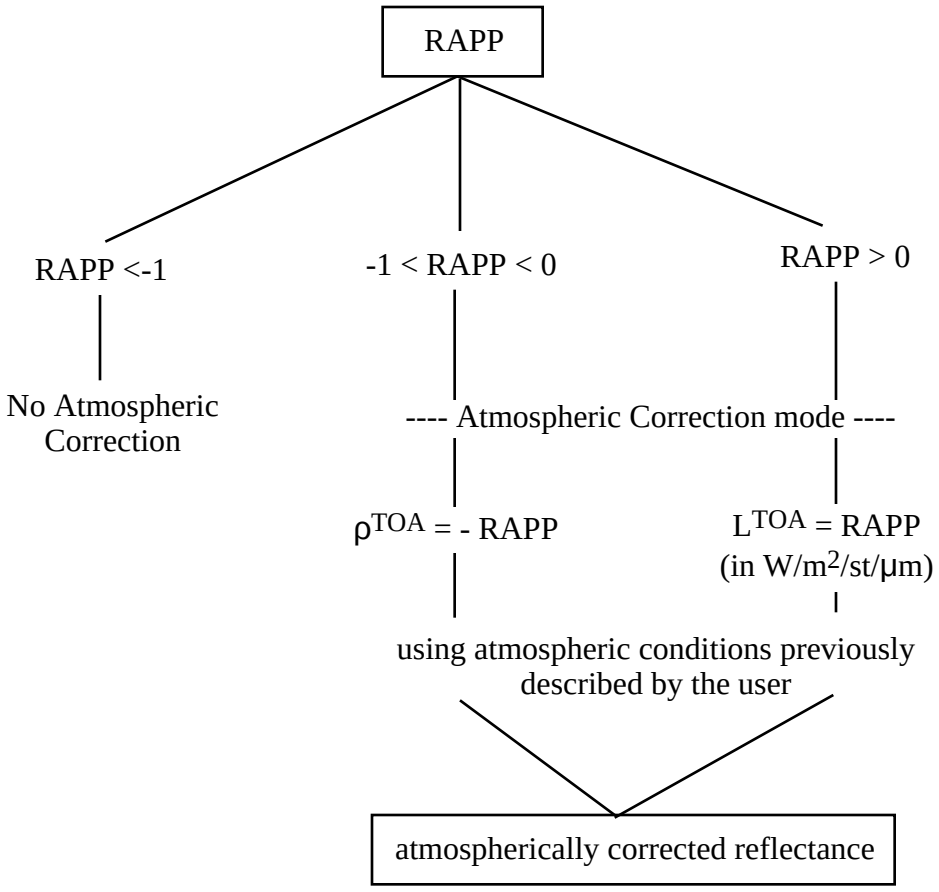

Figure A-9 : Detailed Chart Flow for Atmospheric correction mode

Figure A-10

: Detailed Flow Chart for Discrete Computations of the Scattering Atmospheric Functions, ρ, T(θ) and S

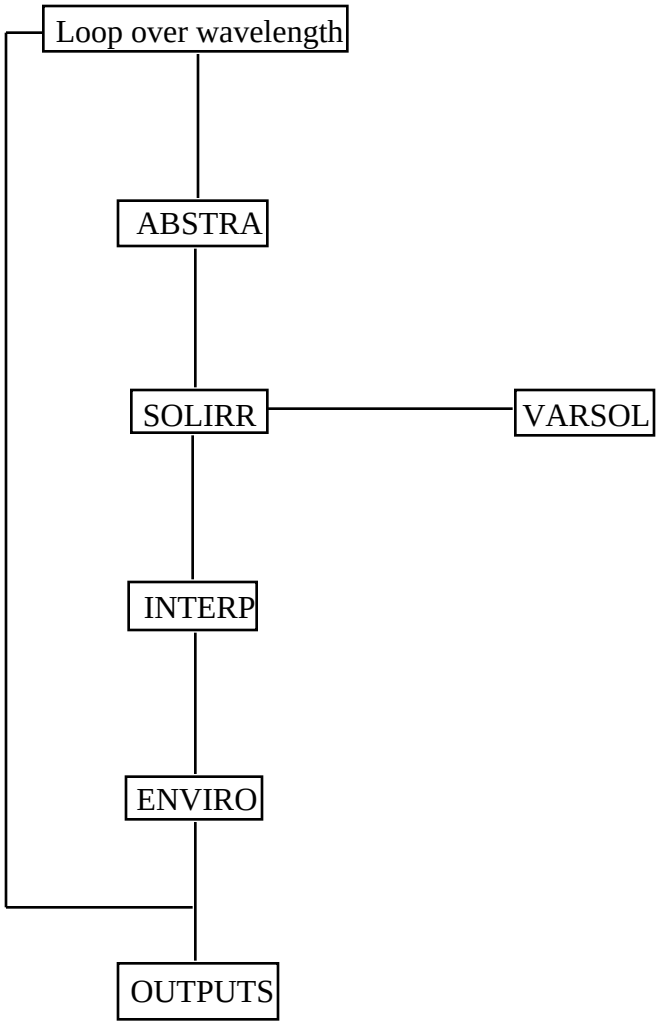

Figure A-11 : Detailed Chart Flow for Spectral Integration

INTEGRATED VALUES OF

Apparent Reflectance: $\frac{\int S(\lambda) E_\lambda \mu_s \rho'_\lambda d\lambda}{\int S(\lambda) E_\lambda \mu_s d\lambda}$

Apparent Radiance: $\frac{1}{\Pi} \frac{\int S(\lambda) E_\lambda \mu_s \rho'_g d\lambda}{\int S(\lambda) d\lambda}$

Total gaseous Transmittance: $\frac{\int S(\lambda) E_\lambda \mu_s T_g^\lambda d\lambda}{\int S(\lambda) E_\lambda \mu_s d\lambda}$

COUPLING AEROSOL-WATER VAPOR

wv above Aer.: $\frac{\int S(\lambda) E_\lambda \mu_s \rho_\lambda^{(1)} d\lambda}{\int S(\lambda) E_\lambda \mu_s d\lambda}$

wv mixed with Aer.: $\frac{\int S(\lambda) E_\lambda \mu_s \rho'_\lambda d\lambda}{\int S(\lambda) E_\lambda \mu_s d\lambda}$

wv under Aer.: $\frac{\int S(\lambda) E_\lambda \mu_s \rho_\lambda^{(2)} d\lambda}{\int S(\lambda) E_\lambda \mu_s d\lambda}$

with $\rho_\lambda^{(1)} = \frac{Tg^\lambda}{Tg^\lambda_{U_{H_2O}}} \left(\rho_{R+A} + (\rho_{R+A} - \rho_R) Tg^\lambda_{U_{H_2O}} + \rho_s^* \right)$

$\rho'_\lambda = \frac{Tg^\lambda}{Tg^\lambda_{U_{H_2O}}} \left(\rho_{R+A} + (\rho_{R+A} - \rho_R) Tg^\lambda_{U_{H_2O}} + \rho_s^* \right)$

$\rho_\lambda^{(2)} = \frac{Tg^\lambda}{Tg^\lambda_{U_{H_2O}}} \left(\rho_{R+A} + \rho_s^* \right)$

where $\rho_s^* = T^\downarrow(\theta_s) T^\uparrow(\theta_v) \frac{\rho_s}{1 - s\rho_s} Tg^\lambda_{U_{H_2O}}$

INTEGRATED NORMALIZED VALUES OF

% Irradiance at ground level

% Direct Irr.: $\frac{\int S(\lambda) E_\lambda \mu_s \frac{e^{-\tau/\mu_s} [1 - < \rho_\lambda > s_\lambda]}{T^\lambda(\theta_s)} d\lambda}{\int S(\lambda) E_\lambda \mu_s d\lambda}$

% diffuse Irr.: $\frac{\int S(\lambda) E_\lambda \mu_s \frac{t_d^\lambda(\theta_s) [1 - < \rho_\lambda > s_\lambda]}{T^\lambda(\theta_s)} d\lambda}{\int S(\lambda) E_\lambda \mu_s d\lambda}$

% Enviro. Irr.: $\frac{\int S(\lambda) E_\lambda \mu_s < \rho_\lambda > s_\lambda d\lambda}{\int S(\lambda) E_\lambda \mu_s d\lambda}$

Reflectance at satellite level

Atm. intrin. ref.: $\frac{\int S(\lambda) E_\lambda \mu_s Tg^\lambda(\theta_s, \theta_v) \rho_\lambda^a d\lambda}{\int S(\lambda) E_\lambda \mu_s d\lambda}$

Envionment ref.: $\frac{\int S(\lambda) E_\lambda \mu_s Tg^\lambda(\theta_s, \theta_v) \frac{T^\lambda(\theta_s) t_d^\lambda(\theta_v) < \rho_\lambda >}{1 - < \rho_\lambda > s_\lambda} d\lambda}{\int S(\lambda) E_\lambda \mu_s d\lambda}$

Target reflectance: $\frac{\int S(\lambda) E_\lambda \mu_s Tg^\lambda(\theta_s, \theta_v) \frac{T^\lambda(\theta_s) e^{-\tau/\mu_v} \rho_\lambda}{1 - < \rho_\lambda > s_\lambda} d\lambda}{\int S(\lambda) E_\lambda \mu_s d\lambda}$

Figure A-12: Description of the outputs (1/3)

INT. ABSOLUTE VALUES OF

Irradiance at ground level

Direct Solar Irr.

$$\frac{\int S(\lambda) E_\lambda \mu_s T_g^\lambda(\theta_s) e^{-\tau/\mu_s} d\lambda}{\int S(\lambda) d\lambda}$$

Atm. diffuse Irr.

$$\frac{\int S(\lambda) E_\lambda \mu_s T_g^\lambda(\theta_s) t_d^\lambda(\theta_s) d\lambda}{\int S(\lambda) d\lambda}$$

Enviro. Irradiance

$$\frac{\int S(\lambda) E_\lambda \mu_s T_g^\lambda(\theta_s) \frac{T^\lambda(\theta_s) < \rho_\lambda >_{s_\lambda}}{1 - < \rho_\lambda >_{s_\lambda}} d\lambda}{\int S(\lambda) d\lambda}$$

Radiance at satellite level (W/m^2/µm)

Atm. intrin. rad.

$$\frac{1}{\Pi} \frac{\int S(\lambda) E_\lambda \mu_s T_g^\lambda(\theta_s, \theta_v) \rho_a^\lambda d\lambda}{\int S(\lambda) d\lambda}$$

Environment radiance

$$\frac{1}{\Pi} \frac{\int S(\lambda) E_\lambda \mu_s T_g^\lambda(\theta_s, \theta_v) \frac{T^\lambda(\theta_s) t_d^\lambda(\theta_v) < \rho_\lambda >_{s_\lambda}}{1 - < \rho_\lambda >_{s_\lambda}} d\lambda}{\int S(\lambda) d\lambda}$$

Target radiance

$$\frac{1}{\Pi} \frac{\int S(\lambda) E_\lambda \mu_s T_g^\lambda(\theta_s, \theta_v) \frac{T^\lambda(\theta_s) e^{-\tau/\mu_v} \rho_\lambda}{1 - < \rho_\lambda >_{s_\lambda}} d\lambda}{\int S(\lambda) d\lambda}$$

(W/m^2/sr/µm)

Int. Function filter (in µm)

$$\int S(\lambda) d\lambda$$

Int. Sol. Spect. (in W/m^2)

$$\int S(\lambda) E_\lambda d\lambda$$

Figure A-12 : Description of the outputs (2/3)

	DOWNWARD	UPWARD	TOTAL
Gas Trans: H_2O, CO_2, O_3, O_2 N_2O, CH_4, CO	$\frac{\int S(\lambda)\mu_s E_\lambda \prod_{i=1}^{7} Tg_i^\lambda(\theta_s)\,d\lambda}{\int S(\lambda)\mu_s E_\lambda\,d\lambda}$	$\frac{\int S(\lambda)\mu_s E_\lambda \prod_{i=1}^{7} Tg_i^\lambda(\theta_v)\,d\lambda}{\int S(\lambda)\mu_s E_\lambda\,d\lambda}$	$\frac{\int S(\lambda)\mu_s E_\lambda \prod_{i=1}^{7} Tg_i^\lambda(\theta_s,\theta_v)\,d\lambda}{\int S(\lambda)\mu_s E_\lambda\,d\lambda}$
Ray. Trans. Aer. Trans. Tot. Trans.	$\frac{\int S(\lambda)\mu_s E_\lambda T_\lambda(\theta_s)\,d\lambda}{\int S(\lambda)\mu_s E_\lambda\,d\lambda}$	$\frac{\int S(\lambda)\mu_s E_\lambda T_\lambda(\theta_v)\,d\lambda}{\int S(\lambda)\mu_s E_\lambda\,d\lambda}$	$\frac{\int S(\lambda)\mu_s E_\lambda T_\lambda(\theta_s)T_\lambda(\theta_v)\,d\lambda}{\int S(\lambda)\mu_s E_\lambda\,d\lambda}$

	Rayleigh	Aerosols	Total
Spherical Albedo	$\frac{\int S(\lambda)\mu_S E_\lambda S^R d\lambda}{\int S(\lambda)\mu_S E_\lambda d\lambda}$	S^A	S^T
Optical Depth	$\frac{\int S(\lambda)\mu_S E_\lambda \tau^R d\lambda}{\int S(\lambda)\mu_S E_\lambda d\lambda}$	τ^A	τ_{A+} τ_R
Reflectance	$\frac{\int S(\lambda)\mu_S E_\lambda \rho^R d\lambda}{\int S(\lambda)\mu_S E_\lambda d\lambda}$	ρ_A	ρ_R + ρ_A
Phase Function	$\frac{\int S(\lambda)\mu_S E_\lambda P^R d\lambda}{\int S(\lambda)\mu_S E_\lambda d\lambda}$	P^A	$\frac{\tau^R P^R + \tau^A P^A}{\tau^R + \tau^A}$
Single Scattering Albedo	*1.0*	ω_0^A	$\frac{\tau^R + \omega_0^A \tau^A}{\tau^R + \tau^A}$

Figure A-10: Description of the outputs (3/3)

APPENDIX II : EXAMPLE OF INPUTS AND OUTPUTS

INPUT FILE

```
0                              (USER'S CONDITIONS)
40.0 100.0 45.0 50.0 7 23
8                              (USER'S MODEL)
3.0   0.35                     (UH2O(G/CM2) ,UO3(CM-ATM))
4                              (AEROSOLS MODEL)
0.25  0.25  0.25  0.25         (% OF:DUST-LIKE,WATER-SOL,OCEANIC,SOOT)
0                              (NEXT VALUE IS THE AER. OPT. THICK. @550)
0.50                           (AERO. OPT. THICK. @550)
-0.2                           (TARGET AT 0.2 km)
-3.3                           (AIRCRAFT AT 3.3 KM ABOVE GROUND LEVEL)
-1.5  -0.35                    (UH2o and UO3 under the plane not avail.)
0.25                           (AERO. OPT. THICK. under the plane @550)
11                             (AVHRR 1 (NOAA 9) BAND)
1                              (GROUND TYPE,I.E. NON UNIFORME SURFACE)
2    1    0.50                 (TARGET,ENV.,RADIUS(KM))
-0.10                          (ATMOSPHERIC CORRECTION OF RAPP=0.10)
```

OUTPUT FILE (1/3)

```
****************************** 6s version 4.1 ******************************
*                       geometrical conditions identity                    *
*                       -------------------------------                    *
*                       user defined conditions                            *
*                                                                          *
* month:  7 day :  23                                                      *
* solar zenith angle:   40.00 deg  solar azimuthal angle:      100.00 deg  *
* view zenith angle:    45.00 deg  view azimuthal angle:        50.00 deg  *
* scattering angle:    146.49 deg  azimuthal angle difference:  50.00 deg  *
*                                                                          *
*                       atmospheric model description                      *
*                       -----------------------------                      *
*           atmospheric model identity :                                   *
*             user defined water content : uh2o= 3.000 g/cm2               *
*             user defined ozone content : uo3 =  .350 cm-atm              *
*             aerosols type identity : user defined aerosols model         *
*                                      .250 % of dust-like                 *
*                                      .250 % of water-soluble             *
*                                      .250 % of oceanic                   *
*                                      .250 % of soot                      *
*           optical condition identity :                                   *
*              visibility :  8.49 km  opt. thick. 550nm :  .5000           *
*                                                                          *
*                       spectral condition                                 *
*                       ------------------                                 *
*                       avhrr 1 (noaa9) value of filter function           *
*                       wl inf=  .530 mic wl sup=  .810 mic                *
*                                                                          *
*                       target type                                        *
*                       -----------                                        *
*                       inhomogeneous ground , radius of target   .500 km  *
*                       target reflectance :                               *
*             spectral clear water reflectance        .045                 *
*                       environmental reflectance :                        *
*             spectral vegetation ground reflectance  .129                 *
*                                                                          *
*                       target elevation description                       *
*                       ----------------------------                       *
*                       ground pressure  [mb]  989.01                      *
*                       ground altitude  [km]  .200                        *
*             gaseous content at target level:                             *
*             uh2o= 3.000 g/cm2               uo3=  .350 cm-atm            *
*                                                                          *
*                       plane simulation description                       *
*                       ----------------------------                       *
*                       plane  pressure  [mb] 657.54                       *
*                       plane  altitude  [km] 3.500                        *
*   atmosphere under plane description:                                    *
*              ozone content              .008                           *
*              h2o   content             2.389                           *
*           aerosol opt. thick. 550nm   .281                               *
*                                                                          *
*                        atmospheric correction activated                  *
*                        --------------------------------                  *
*                       input apparent reflectance :   .100                *
*                                                                          *
****************************************************************************
```

OUTPUT FILE (2/3)

```
*******************************************************************************
*                                                                             *
*                          integrated values of  :                            *
*                          -----------------------                            *
*       apparent reflectance .0442    appar. rad.(w/m2/sr/mic)   17.028       *
*                    total gaseous transmittance   .932                       *
*                                                                             *
*******************************************************************************
*                                                                             *
*                          coupling aerosol -wv  :                            *
*                          -----------------------                            *
*           wv above aerosol :  .044     wv mixed with aerosol :  .044        *
*                         wv under aerosol :  .044                            *
*                                                                             *
*                          int. normalized  values  of  :                     *
*                          ---------------------------                        *
*                       % of irradiance at ground level                       *
*     % of direct  irr.    % of diffuse irr.    % of enviro. irr              *
*                 .792                 .203                .005               *
*                        reflectance at satellite level                       *
*     atm. intrin. ref.   environment ref.  target reflectance                *
*                 .020                 .014                .014               *
*                                                                             *
*                          int. absolute values of                            *
*                          -----------------------                            *
*                      irr. at ground level (w/m2/mic)                        *
*     direct solar irr.    atm. diffuse irr.    environment  irr               *
*             617.585             157.626             3.673                   *
*                      rad at satel. level (w/m2/sr/mic)                      *
*     atm. intrin. rad.    environment rad.    target radiance                *
*                7.605               5.246               5.525                *
*                                                                             *
*                                                                             *
*           int. funct filter (in mic)              int. sol. spect (in w/m2) *
*                .1174545                                185.589              *
*                                                                             *
*******************************************************************************
```

OUTPUT FILE (3/3)

```
**************************************************************************
*                                                                        *
*                          integrated values of  :                       *
*                          -----------------------                       *
*                                                                        *
*                             downward        upward          total      *
*      global gas. trans. :     .94431         .98066         .93234      *
*      water   "     "    :     .98573         .98623         .97592      *
*      ozone   "     "    :     .96462         .99907         .96373      *
*      co2     "     "    :    1.00000        1.00000        1.00000      *
*      oxyg    "     "    :     .99344         .99533         .99179      *
*      no2     "     "    :    1.00000        1.00000        1.00000      *
*      ch4     "     "    :    1.00000        1.00000        1.00000      *
*      co      "     "    :    1.00000        1.00000        1.00000      *
*                                                                        *
*                                                                        *
*      rayl.  sca. trans. :     .96436         .93710         .90371      *
*      aeros. sca.   "    :     .70714         .81147         .57382      *
*      total  sca.   "    :     .67814         .80093         .54315      *
*                                                                        *
*                                                                        *
*                                                                        *
*                             rayleigh       aerosols         total      *
*                                                                        *
*      spherical albedo   :     .04934         .04532         .06365      *
*      optical depth total:     .05550         .41782         .47332      *
*      optical depth plane:     .01848         .23471         .25320      *
*      reflectance        :     .01081         .01274         .02081      *
*      phase function     :    1.26026         .30427         .41637      *
*      sing. scat. albedo :    1.00000         .48167         .54245      *
*                                                                        *
*                                                                        *
**************************************************************************



**************************************************************************
*                        atmospheric correction result                   *
*                        -----------------------------                   *
*                input apparent reflectance      :  .100                 *
*                measured radiance [w/m2/sr/mic] : 38.529                *
*                atmospherically corrected reflectance :  .156           *
*                coefficients xa xb xc                 : .00513 .04109 .06365 *
*           y=xa*(measured radiance)-xb ; acr=y/(1.+xc*y)                *
**************************************************************************
```